

**Charging and Discharging Characterization of Novel
Combined Sensible-Latent Heat TES System by
Experimental Investigations for Medium Temperature
Applications**



By

Malik Sarmad Zahid

Reg # 00000320982

Session 2019-2021

Supervised by

Dr. Naveed Ahmed

**A Thesis Submitted to the US Pakistan Centre for Advanced
Studies in Energy in partial fulfillment of the requirements of**

the degree of

MASTER of SCIENCE in

THERMAL ENERGY ENGINEERING

US-Pakistan Centre for Advanced Studies in Energy (USPCAS-E)

National University of Sciences and Technology (NUST)

H-12, Islamabad 44000, Pakistan

May 2022

THESIS ACCEPTANCE CERTIFICATE

Certified that final copy of MS/MPhil thesis written by **Mr. Malik Sarmad Zahid** (Registration No. 00000320982), of USPCAS-E has been vetted by undersigned, found complete in all respects as per NUST Statues/Regulations, is within the similarity indices limit, and is accepted as partial fulfillment for the award of MS/MPhil degree. It is further certified that necessary amendments as pointed out by GEC members of the scholar have also been incorporated in the said thesis.

Signature: _____

Name of Supervisor Dr. Naveed Ahmed

Date: _____

Signature (HoD TEE): _____

Date: _____

Signature (Dean/Principal): _____

Date: _____

Certificate

This is to certify that work in this thesis has been carried out by **Mr. Malik Sarmad Zahid** and completed under my supervision in US-Pakistan Center for Advanced Studies in Energy (USPCAS-E), National University of Sciences and Technology, H-12, Islamabad, Pakistan.

Supervisor:

Dr. Naveed Ahmed
USPCAS-E
NUST, Islamabad

GEC member 1:

Prof. Dr. Adeel Waqas
USPCAS-E
NUST, Islamabad

GEC member 2:

Dr. Majid Ali
USPCAS-E
NUST, Islamabad

GEC member 3:

Dr. Mariam Mahmood
USPCASE
NUST, Islamabad

HOD-TEE:

Dr. Majid Ali
USPCAS-E
NUST, Islamabad

Principal:

Prof. Dr. Adeel Waqas
USPCAS-E
NUST, Islamabad

Dedication

I would like to wholeheartedly dedicate my thesis to my beloved parents, who have been a constant source of inspiration and strength and continuously provided their moral, spiritual, and emotional support. To my brothers, mentor, and friends who shared their words of advice and encouragement to help me finish this study.

Abstract

Efficient and economical thermal energy storage (TES) system can effectively reduce mismatch between seasonal energy supply and demand. The single tank type thermocline TES has been investigated as economical alternative for medium temperature applications. However, key disadvantages of this design are quick degradation of thermocline thickness, thermal ratcheting and drop of temperature at outlet section during discharging. To overcome these issues, a new type of structured hybrid sensible-latent design is developed in this research. The focus of the present work is to experimentally investigate the charge and discharge performance of the proposed TES system and it is designed by incorporating the sensible heat concrete block with axial holes placed in between multilayers of PCMs (D- mannitol and adipic acid). Charge and discharge experiments are performed to study the effect of hybrid structured concrete and multilayer PCM's configuration on thermocline temperature profiles, stratification number, total energy stored and retained by storage medium, effective charge and discharge efficiency, utilization ratio. The relative experimental study is developed for four configurations, i.e., multilayered sensible heat concrete with PCM (MLSPCM), two uni-layered sensible concrete with PCM (SLSPCM-1 and SLSPCM-2) arrangements and single sensible heat concrete block (SSCB) arrangement. The results show that effective discharge efficiency and storage capacity of MLSPCM, SLSPCM-1, SLSPCM-2 and SSCB are 87%, 85%, 86%, 79% and 12.53kWhr, 10.37kWhr, 9.96kWhr, 6.23kWhr, respectively. Moreover, the charging and discharging behavior of MLSPCM is further characterized at different mass flow rates to study the effect on thermocline thickness formation, effective discharge time and amount of energy extracted from storage medium. The present study shows that use of multilayers of PCM with suitable melting and solidification temperature together with low-cost sensible concrete, is viable and economical TES solution for medium temperature applications.

Keywords: Thermal energy storage; medium temperature; thermocline temperature profiles; hybrid multilayered sensible-latent design; structured sensible medium.

Table of Contents

Abstract.....	v
List of figures.....	ix
List of tables.....	xi
List of journal papers/conference papers.....	xii
List of abbreviations.....	xiii
Chapter # 1 Introduction.....	1
1.1 Background.....	1
1.1.1 Energy storage	1
1.1.2 Thermal energy storage	1
1.1.3 Types of thermal energy storage	2
1.1.4 Combined sensible-latent thermal energy storage.....	3
1.2 Research objectives.....	3
Summary.....	5
References.....	6
Chapter # 2 Literature Review.....	7
2.1 Problems of conventional energy resources.....	7
2.2 Integrating thermal energy storages with renewable energy resources.....	7
2.3 Thermal energy storages for medium temperature applications.....	8
2.3.1 Sensible heat storage.....	8
2.3.2 Latent heat storage.....	8
2.4 Hybrid multilayered thermal energy storage unit.....	9

Summary.....	11
References.....	12
Chapter # 3 Experimental Methodology.....	14
3.1 Methodology.....	14
3.2 Proposed TES designs.....	15
3.3 Experimental setup.....	17
3.3.1 Latent heat storage medium.....	18
3.3.2 Sensible heat storage medium.....	20
3.3.3 Heat transfer fluid.....	21
3.4 Experimental procedure	22
3.5 Arrangement of thermocouples in TES and buffer tank.....	24
3.6 Thermal performance evaluation.....	25
3.6.1 Energy supplied and removed by HTF.....	25
3.6.2 Energy gain and recovered by storage medium.....	25
3.6.3 Discharge efficiency.....	26
3.6.4 Charge efficiency.....	26
3.6.5 Fraction of heat retained by storage medium.....	27
3.6.6 Liquid fraction.....	27
3.6.7 Stratification number.....	27
3.6.8 Thermocline thickness.....	28
Summary.....	29
References.....	30
Chapter # 4 Results & Discussions.....	32

4.1 Thermal performance of TES systems.....	32
4.1.1 Thermocline temperature profiles.....	32
4.1.2 Temperature profile of fluid at center.....	36
4.1.3 Comparative temperature profile of PCM, SCB and HTF.....	38
4.1.4 Stratification number.....	41
4.1.5 Comparative temperature profile of fluid at outlet section.....	43
4.1.6 Variation of liquid fraction.....	46
4.2 Performance parameters for proposed TES systems.....	48
4.2.1 Thermal energy transferred and removed by HTF.....	48
4.2.2 Thermal energy accumulated and retrieved by storage medium.....	50
4.2.3 Comparative charge and discharge efficiency.....	52
4.3 Thermal performance characterization of MLSPCM.....	54
4.3.1 Thermocline temperature profiles at different mass flow rates.....	55
4.3.2 Temperature profiles of fluid and SCB at center.....	57
4.3.3 Fluid temperature at outlet for changing mass flow rates.....	59
4.3.4 Charge and discharge efficiency at different mass flow rates.....	60
4.3.5 Energy removed by HTF during discharging.....	60
4.3.6 Fraction of energy retained by PCM and SCB.....	60
4.3.7 Thermocline thickness for different mass flow rates.....	61
Summary.....	62
Chapter # 5 Conclusions & Recommendations.....	63
5.1 Conclusions.....	63
5.2 Future recommendations.....	64

List of Figures

Figure 1.1: Type of TES systems.....	2
Figure 1.2: Flow chart of thesis.....	4
Figure 3.1: Flow chart of experiment.....	15
Figure 3.2: 2D sketch of arrangement of PCM and SCB for proposed TES configurations a) MLSPCM b) SLSPCM-1 c) SLSPCM-2 d) SSCB.....	16
Figure 3.3: Experimental setup.....	18
Figure 3.4: Encapsulated PCM arrangements in rows.....	20
Figure 3.5: Concrete block with radial and axial holes.....	21
Figure 3.6: Schematic of experimental setup.....	23
Figure 3.7: Storage tank with thermocouples in radial and axial direction a) outer view b) inner view of TES unit.....	25
Figure 4.1: Distribution of temperature profiles along axial height of tank a) MLSPCM b) SLSPCM-1 c) SLSPCM-2 d) SSCB during charging.....	34
Figure 4.2: Distribution of temperature profiles along axial height of tank a) MLSPCM b) SLSPCM-1 c) SLSPCM-2 d) SSCB during discharging.....	35
Figure 4.3: Comparative temperature profiles of fluid at $x=H/2$ for four configurations a) charging b) discharging.....	37
Figure 4.4: (a) Comparative temperature profiles of PCM and HTF b) Comparative temperature profiles of SCB and HTF for four configurations during charging.....	39
Figure 4.5: (a) Comparative temperature profiles of PCM and HTF b) Comparative temperature profiles of SCB and HTF for four configurations during discharging.....	40
Figure 4.6: Stratification number for proposed TES designs w.r.t time.....	43

Figure 4.7: Temperature of fluid w.r.t time at outlet section a) during charge b) discharge process.....45

Figure 4.8: Variation of liquid fraction with time a) charge b) discharge process...47

Figure 4.9: Thermal energy a) supplied during charge b) removed by HTF during discharge process.....49

Figure 4.10: Total energy a) stored by storage medium during charge b) recovered during discharge process for proposed TES designs.....51

Figure.4.11: Comparative charge and discharge efficiencies for four different configurations.....54

Figure.4.12: Variation of temperature profile of MLSPCM storage medium along axial height of tank a) charging b) discharging process.....56

Figure 4.13: Comparative fluid temperature profile at $x=H/2$ as a function of charging time for different inlet mass flow rates.....57

Figure 4.14: Comparative temperature profiles of HTF and SCB at $x = H/2$ w.r.t discharging time for different inlet mass flow rates.....58

Figure 4.15: Fluid temperature at outlet section for a) charging b) discharge cycle...59

Figure 4.16: Energy recovered by HTF during discharging for different fluid flow rate.....60

Figure 4.17: Variation of thermocline thickness w.r.t discharge time at different flow rates.....61

List of Tables

Table 3.1: Specifications of TES tank.....	17
Table 3.2: Properties of PCM	19
Table 3.3: Specifications of latent section.....	19
Table 3.4. Properties of SCB.....	20
Table 3.5. Specifications of sensible storage section.....	21
Table 3.6: Properties of HTF.....	22
Table 3.7: Positions of SCB and PCM for proposed designs.....	22
Table 4.1: Performance parameters for four configurations.....	51
Table 4.2: Performance parameters at different inlet mass flow rates.....	58

List of journal papers/conference papers

Charging and discharging characterization of novel combined sensible-latent heat TES system by experimental investigation for medium temperature application

Malik Sarmad Zahid^a, Naveed Ahmed^{*a}, Mumtaz A Qaisrani^b, Mariam Mahmood^a, Majid Ali^a, Adeel Waqas^a

^aUS Pakistan Centre for Advanced Studies in Energy (USPCASE), National University of Sciences & Technology (NUST), H-12 Sector, Islamabad, Pakistan.

^bDepartment of Mechanical Engineering, Khwaja Fareed University of Engineering and Information Technology, Rahim Yar Khan 64200, Pakistan

*Corresponding author. E-mail address: Naveed.ahmed@uspcase.nust.edu.pk (Naveed Ahmed).

Journal: Energy storage

Paper Status: Under Review

List of Abbreviations

$T_{f, in}$	Inlet temperature of HTF ($^{\circ}\text{C}$)
$T_{f, out}$	Outlet temperature of HTF ($^{\circ}\text{C}$)
T_{PCM}	Temperature of latent storage ($^{\circ}\text{C}$)
T_m	Melting temperature ($^{\circ}\text{C}$)
T_i	Initial temperature ($^{\circ}\text{C}$)
T_s	Solidus temperature ($^{\circ}\text{C}$)
T_l	Liquidus temperature ($^{\circ}\text{C}$)
T_h	Critical hot temperature ($^{\circ}\text{C}$)
T_c	Critical cold temperature ($^{\circ}\text{C}$)
T_{tc}	Thermocline thickness (m)
H_{PCM}	Height of latent storage (m)
t	Thickness (m)
D	Diameter of tubes (m)
D_f	Diameter of fins (m)
D_t	Diameter of tank (m)
H_t	Height of tank (m)
R	Radius of tank (m)
R_{PCM}	Radius of latent storage (m)
k	Thermal conductivity (W/m K)
H_{SCB}	Height of concrete block (m)
D_{SCB}	Diameter of concrete block (m)

V_{SCB}	Volume of concrete (m^3)
V_{PCM}	Volume of latent storage (m^3)
$C_{p,s}$	Specific heat capacity of solid (J/kg K)
$C_{p,l}$	Specific heat capacity of liquid (J/kg K)
L_f	Latent heat of fusion of PCM
Q_{sup}	Energy transferred by HTF during charging (W)
Q_{rec}	Energy recovered by HTF during discharging (W)
$Q_{g, sen}$	Energy stored by sensible material during charging (kJ)
$Q_{g, latent}$	Energy stored by latent storage during charging (kJ)
$Q_{rec, sen}$	Energy recovered by sensible material during discharging (kJ)
$Q_{rec, latent}$	Energy recovered by latent storage during discharging (kJ)
$E_{f, PCM}$	fraction of heat retained by latent storage
$E_{f, SCB}$	fraction of heat retained by sensible storage
S.N	Stratification number
MLSPCM	Multilayer sensible latent storage
SLSPCM	Single layer sensible latent storage
SSCB	Single sensible storage
PCM-1	D- mannitol
PCM-2	Adipic acid
Greek letters	
ρ	Density (kg/m^3)
μ	Dynamic viscosity ($kg/m s$)
ε	Porosity

η_c Charge efficiency

η_d Discharge efficiency

ω Liquid fraction

Subscripts

PCM phase change material

HTF heat transfer fluid

SCB sensible concrete block

Chapter 1

Introduction

1.1 Background

In the recent century, the world's population has increased at faster rate which increases the demand of energy. In the past the most of energy demands are fulfilled using conventional resources i.e, coal, furnace oil[1]. The continuous depletion of traditional resources increases the research and development of alternative energy resources. Renewable energy resources are appearing to be the brightest path to bring flexibility, sustainability, and effectiveness in the global energy market. It is an undeniable substitute for replacement of fossil fuels.

1.1.1 Energy storage

Energy storage systems are very important to the success of any intermittent energy source i.e., storing of solar energy is necessary especially when it is not much available namely in winter. Energy storage systems can effectively reduce the imbalance between energy supply and demand. These systems decrease the carbon emissions and maximize the energy utilization. Energy demands in commercial and industrial sector varies and peak hours demand is very difficult to meet. Usually, peak hours demand is generally met by using conventional sources. Energy storage systems are best alternative method of supplying peak energy in most of industries by storing the waste heat.

1.1.2 Thermal energy storage

Thermal energy storage (TES) systems store the available heat for use in different applications, such as space heating, process heating and for supply of hot water for domestic applications[2]. Types of thermal energy storage are presented in figure 1.2.

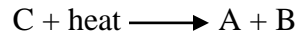
1.1.3 Types of Thermal energy storage

Thermal energy can be stored in the form of sensible, latent heat, combination of sensible and latent and thermochemical heat energy.

Sensible heat by increasing or decreasing the temperature of storage medium. Water, concrete, bricks are used as sensible heat storage materials[3].

Latent heat by changing the phase of storage material[4].

Thermochemical energy by chemical reaction between substances. Energy is recovered in reverse chemical reaction. These storages have high storage density to store more energy using less storage substance.



Where C is and thermochemical substance which absorb heat and converted to A and B. A may be any hydroxide, carbonate and B may be water, ammonia[5].

Hybrid sensible-latent heat by both the phase change and without phase change of storage media. Types of thermal energy storage are presented in Fig.1.1.

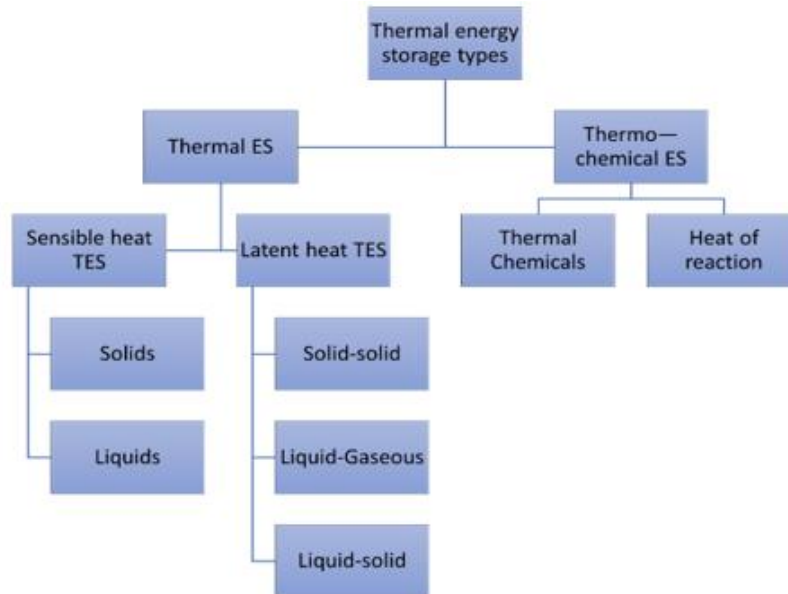


Fig. 1.1 Types of thermal energy storage

1.1.4 Combined sensible-latent thermal energy storage

Hybrid sensible-latent TES unit consists of cheap naturally occurring material and phase change material (PCM) in a single tank. This system contains either multilayers of PCM or single layer of PCM. Most used sensible storage materials are rocks, sand and bricks. In multilayered PCM configuration, PCM's are arranged in order of decreasing melting temperatures along the axial height of tank to increase its storage capacity and utilization of energy during discharging. Combined TES unit have certain advantages over sensible and latent storage systems like

- High storage density which reduces the overall volume of storage.
- Better thermocline performance i.e., thermal gradient is maintained in TES tank.
- Stabilization of outlet temperature of fluid used for certain application.

But hybrid design exhibits low storage time and high thermal losses which needs more focus.

1.2 Research objectives

The present study aims to propose the most efficient and economical TES unit for medium temperature applications by comparing charging and discharging behavior of multilayered hybrid TES system with uni layered combined TES unit and only sensible heat storage unit. Moreover, the study unveils the impact of change in fluid mass flow rate at inlet on thermal behavior of multilayered combined TES unit.

The main objectives of this study are

- Design of hybrid TES systems for medium temperature range
- Prototyping and experimentation to characterize the thermal behavior of the proposed TES design
- Identification of best suitable TES configuration based on various thermal performance parameters like thermocline temperature profile, energy storage and removed by storage material, charge, and discharge efficiency etc.

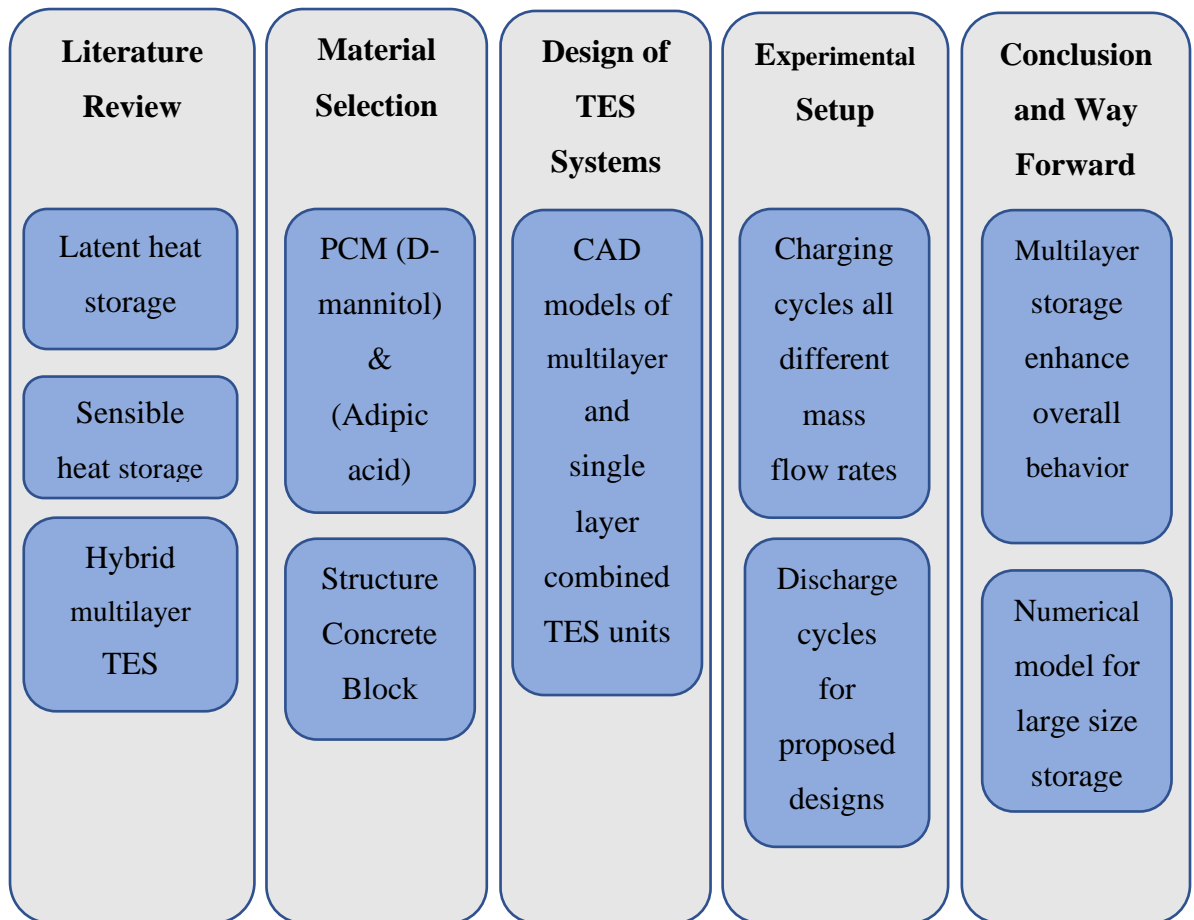


Fig. 1.2 Flow chart of thesis

Summary

In this chapter, the importance of energy storage with renewable energy source is discussed. Then a brief introduction of thermal energy storage and its types is presented. An introduction of hybrid multilayered TES and its advantages and disadvantages are also presented. The scope of the study and the research objectives of present study are also discussed in the chapter.

References

1. Oliveira, Armando C., The energy shift: towards a renewable future. 2007. **2**(3): p. 289-299.
2. Gil, Antoni Medrano, Marc Martorell, Ingrid Lazaro, Ana Dolado, Pablo Zalba, Belen Cabeza, Luisa F., State of the art on high temperature thermal energy storage for power generation. Part 1—Concepts, materials and modellization. 2010. **14**(1): p. 31-55.
3. Koçak, Burcu, Ana Ines Paksoy, Fernandez, and Halime., Review on sensible thermal energy storage for industrial solar applications and sustainability aspects. 2020. **209**: p. 135-169.
4. Elias, Charalambos N Stathopoulos, and Vassilis N., A comprehensive review of recent advances in materials aspects of phase change materials in thermal energy storage. 2019. **161**: p. 385-394.
5. H Abedin, Ali A Rosen, and Marc., A critical review of thermochemical energy storage systems. 2011. **4**(1).

Chapter 2

Literature Review

2.1 Problems of conventional energy resources

Conventional methods of power generation have adverse effect on the environment. With the continuous reduction of traditional fuels, it is time to decrease the use of end the conventional methods and to shift towards the renewable sources of energy. The research for alternative fuels utilization is ongoing rapidly to prevent the environmental issues like global warming as well as to meet the continuously increasing power demand of the world.

2.2 Integrating TES with renewable energy resources

Solar energy plays a key role to meet the thermal energy demand of various applications like space heating. The major issue with this renewable energy source is high cost and availability of solar energy. To overcome these barriers efficient and economical TES system can be included with solar thermal energy unit. TES system stores the energy when available in excess quantity and supply it when demand is high to reduce the imbalance between energy supply and demand. Nandi et al. [1] compared different high temperature sensible storages for solar power plant with capacity of 50MW. Among storage mediums concrete and ceramic showed better thermal performance. Steinmann et al. [2] examined different storage mediums for direct steam generation using solar energy. It is noticed that integrating latent storage unit increases storage capacity and decreases the pressure drop of steam during discharging. Enibe designed and studied performance of solar air heater with PCM for plants and other crops that are not directly heated by sunlight. He tested system without any load and observed that maximum temperature of heated air was 15K with efficiency of 50%. Chaurasia et al. compared latent heat and sensible heat storage based solar energy storage system for supply of hot water. They used paraffin wax as

PCM and water as sensible storage media. It is concluded that system with PCM as storage supplied more water at required high temperature.

2.3 Thermal energy storages for medium temperature applications

In a TES system the energy is stored as sensible heat, latent heat, or combination of both sensible and latent heat.

2.3.1 Sensible heat storage

In sensible storage systems energy is stored by raising the internal temperature of medium. Cheng et al. [3] experimentally and numerically compared the heat transfer performance of cascaded storage unit with single stage storage unit for cold storage applications. They concluded that using cascaded unit results in reduction in charging time and charging rates. Ming Wu et al. [4] compared the thermal performance of four different sensible TES units using concrete as storage media for high and medium temperature applications. It is noticed that packed bed configuration show better thermocline performance and highest discharge efficiency while channel type structure exhibits poor performance. Strasser et al. [5] compared the structured concrete thermocline TES tank and packed bed structure. It is found that thermal stresses developed in packed bed design when the temperature is increased from low to medium range which makes it less feasible.

2.3.2 Latent heat storage

Ashmore et al. [6] performed experiment to compare the thermal stratification, energy accumulation rate of 3-stage cascaded PCM with single and 2-stage PCM configurations during charging for medium temperature application. It is noticed that 3-stage cascaded PCM configuration has 4%, 26% and 30% higher stratification performance as compared to other designs. Also using three layers of different PCM have high energy storage rate. An experimental study is performed by Zhongbin Zhang et al. [7] to study the effect of number of stages of PCM's, different fractions of PCM layers and melting temperature on heat storage performance of latent heat storage system. They selected four different kind of paraffin wax with different melting temperatures as latent heat storage medium. The results show that using more high melting PCM's, the heat storage and release

capacity and exergy efficiency increases. But it will increase the charging and discharging time. Further, it is noticed that more number of stages improved the heat storage performance. Piero et al. [8] compared TES units containing single layer PCM and cascaded layer PCM configurations using D-mannitol and hydroquinone for temperature range of 150°C-200°C. It is concluded with multi-layer PCM TES concept thermal performance of storage system is enhanced.

2.4 Hybrid multilayered TES unit

Sensible heat TES mediums are simple, low cost, easily available but are not too much effective due to low energy storage density and decrease in temperature at the end of discharging[9]. The latent heat TES systems have high energy storage density, less thermal energy losses and isothermal operation during charging and discharging. LHTES can store more heat than SHTES but still are not much effective due high cost of storage medium, effect of subcooling and low conductivity[10]. The issues related to SHTES and LHTES can be reduced by combining both phase change material and sensible heat storage material in a single tank.

Nallusamy et al. [11] experimentally studied the charging and discharging characteristics of combined sensible and single layer latent heat TES system using water as both HTF and sensible storage medium. They compared the thermal characteristics of combined TES with simple sensible heat TES system and concluded that hybrid configuration gives better thermal performance than simple SHTES. Mawire et al. [12] compared the charging performance of latent heat TES and combined TES configurations and noticed that thermal performance is enhanced by placing the PCM above the low-cost sensible storage medium, also the energy storage is enhanced by using the hybrid configuration.

Zanganeh et al. [13] performed experiments and developed the simulation model to study the effect the placing the PCM above the rocks as sensible heat storage medium, for high temperature applications. It is concluded that outlet temperature of HTF is stabilized during discharging process. Naveed Ahmed et al. [14] compared the thermal behavior of four different configurations and concluded that using the multilayer PCM with the low cost naturally occurring sensible storage medium can enhance the exergy efficiency,

utilization ratio and also stabilize the temperature during the discharging cycles. Christoph Zauner et al. [15] experimentally studied the effect of changing mass flow rates and fluid inlet temperatures on charge and discharge performance of hybrid sensible and latent heat storage configuration. They utilized high density polyethylene (HDPE) as PCM and thermal oil as sensible storage and heat transfer fluid. The numerical simulations were also performed to study the heat transfer in detail. D. Lafri et al. [16] performed experiment using two different configurations of mixed storage (sensible and latent). They examined the phase change phenomenon and thermal stratification of PCM. It is noticed that arranging the storage medium circumferentially accelerates the melting as compared to storage medium placed at the center. An experimental study is performed by C. Suresh et al. [17] to examine the effect of changing the volume of PCM on energy storage by medium, energy recovered by HTF, charge and discharge time of hybrid TES system. They proposed that higher volume fractions of 80% and 60% have better thermal performance as compared to low volume fractions (40% and 20%).

The literature study concludes that most of the authors focused on hybrid configuration using the packed bed and PCM. The literature study also shows that no work has been done on using the stable concrete structure as sensible heat storage with the multilayer PCM in single tank to overcome the disadvantages of alone latent and sensible storages.

Summary

This chapter includes the literature review about energy storage systems combined with solar thermal systems. Several TES systems for medium temperature application are discussed and hybrid multilayered TES systems is proposed as more viable TES alternative. Advantages and disadvantages of storage incorporation in solar energy systems are also elaborated.

References

1. Nandi, Bhaskar Rahul Bandyopadhyay, Santanu Banerjee, and Rangan., Analysis of high temperature thermal energy storage for solar power plant. in 2012 IEEE Third International Conference on Sustainable Energy Technologies (ICSET). 2012. IEEE.
2. Steinmann, Wolf-Dieter Eck, and Marcus., Buffer storage for direct steam generation. 2006. **80**(10): p. 1277-1282.
3. Cheng, Xiwen Zhai, and Xiaoqiang., Thermal performance analysis and optimization of a cascaded packed bed cool thermal energy storage unit using multiple phase change materials. 2018. **215**: p. 566-576.
4. Wu, Ming Li, Mingjia Xu, Chao He, Yaling Tao, Wenquan., The impact of concrete structure on the thermal performance of the dual-media thermocline thermal storage tank using concrete as the solid medium. 2014. **113**: p. 1363-1371.
5. Strasser, Matthew N Selvam and R Paneer., A cost and performance comparison of packed bed and structured thermocline thermal energy storage systems. 2014. **108**: p. 390-402.
6. Mawire, Ashmore Ekwomadu, Chidiebere S Shobo, Adedmola B., Experimental charging characteristics of medium-temperature cascaded packed bed latent heat storage systems. 2021. **42**: p. 103067.
7. Zhang, Zhongbin Ci., Zhongqiu Zhang, and Tianyu., Heat-storage performance optimization for packed bed using cascaded PCMs capsules. 2021. **42**(5): p. 1-20.
8. Peiró, Gerard Gesia, Jaume Miro, Laia Cebaza, Luisa F., Experimental evaluation at pilot plant scale of multiple PCMs (cascaded) vs. single PCM configuration for thermal energy storage. 2015. **83**: p. 729-736.
9. Elias, Charalambos N Stathopoulos, and Vassilis N., A comprehensive review of recent advances in materials aspects of phase change materials in thermal energy storage. 2019. **161**: p. 385-394.

10. Alva, Guruparasad Liu, Lingkun Huang, Xiang Fang, Guiyin., Thermal energy storage materials and systems for solar energy applications. 2017. **68**: p. 693-706.
11. Nallusamy, N Sampath, and S Velraj., Experimental investigation on a combined sensible and latent heat storage system integrated with constant/varying (solar) heat sources. 2007. **32**(7): p. 1206-1227.
12. Mawire, Ashmore Lentswe, Katlego Shobe, Adedamola., Performance comparison of a latent heat and combined thermal energy systems during charging. in 2018 International Conference on Renewable Energy and Power Engineering (REPE). 2018. IEEE.
13. Zanganeh, Giw Khanna, Raghav Walser, Christoph Pedretti, Andrea Haselbacher, Andreas Stienfield, Aldo., Experimental and numerical investigation of combined sensible–latent heat for thermal energy storage at 575 C and above. 2015. **114**: p. 77-90.
14. Ahmed, N Elfeky, Ke Lu, Lin Wang, QW., Thermal performance analysis of thermocline combined sensible-latent heat storage system using cascaded-layered PCM designs for medium temperature applications. 2020. **152**: p. 684-697.
15. Zauner, Christoph Hengstberger, Florian Morzinger, Benjamin Hofmann, Rene Walter, Heimo., Experimental characterization and simulation of a hybrid sensible-latent heat storage. 2017. **189**: p. 506-519.
16. Lafri, D Semmar, D Hamid, A Ouzzane., Experimental investigation on combined sensible and latent heat storage in two different configurations of tank filled with PCM. 2019. **149**: p. 625-632.
17. Suresh, C Saini, and RP., Experimental study on combined sensible-latent heat storage system for different volume fractions of PCM. 2020. **212**: p. 282-296.

Chapter 3

Experimental Methodology

3.1 Methodology

The methodology used for the present study is.

1. First selection of suitable sensible, latent storage tank material according to requirement of application.
2. Designing of TES unit i.e arrangement of storage mediums in tank, which is divided into four different types of design, MLSPCM, SLSPCM-1, SLSPCM-2 and SSCB.
3. Fabrication of energy storage and buffer storage (for storage of HTF)
4. Proper insulation of both tanks and heating of HTF to the required temperature
5. Charging and discharging experiments at different flow rates for the proposed design models
6. Finally, selection of suitable and efficient TES design.

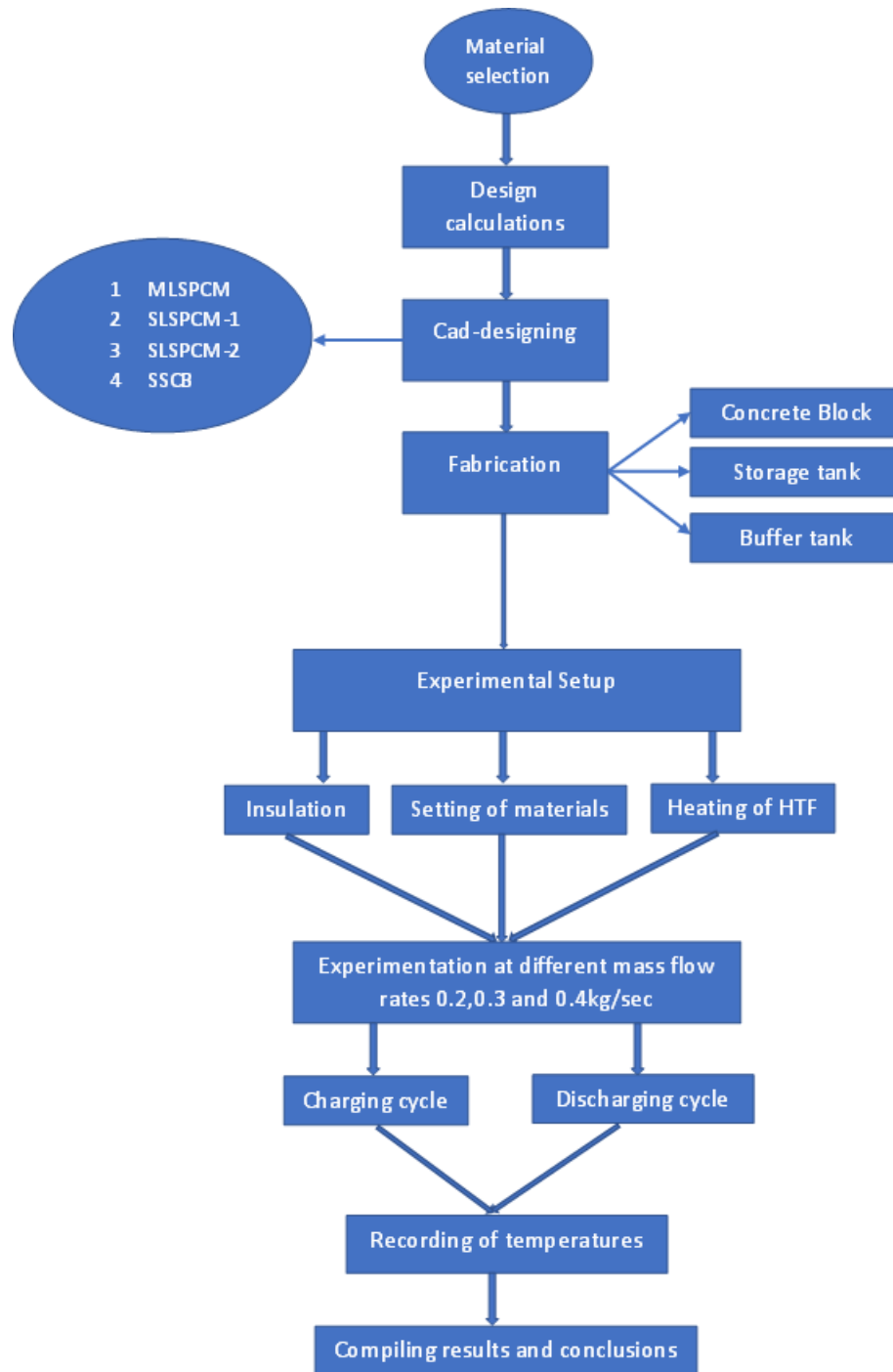


Fig. 3.1. Research methodology

3.2 Proposed TES designs

Present research includes the comparative charge and discharge study of four different designs. MLSPCM consist of concrete block at the center and multilayers of PCM's at

top and bottom section. SLSPCM-1 and SLSPCM-2 designs have single layer of PCM at the top of concrete block. While SSCB contain only sensible media in TES tank.

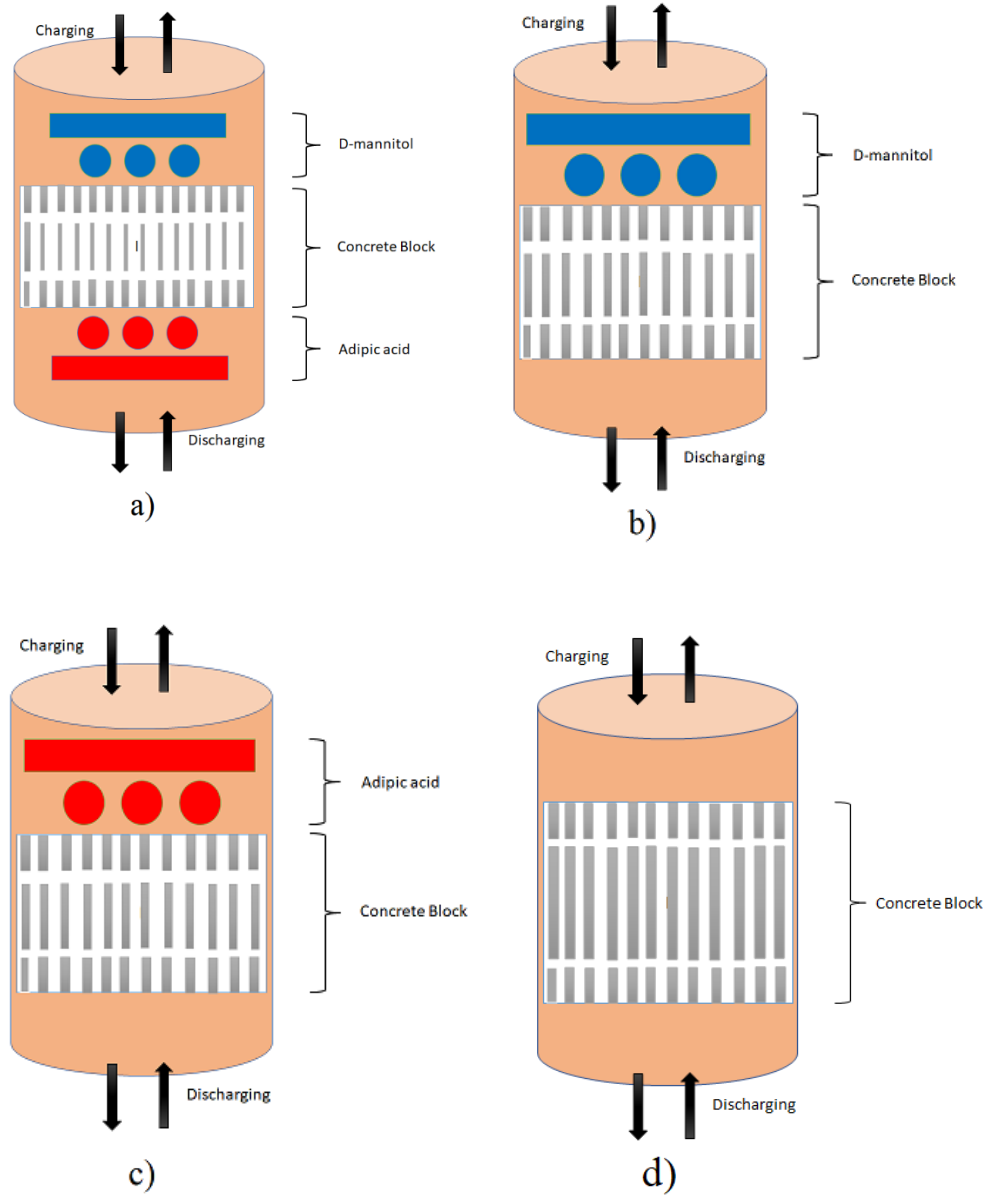


Fig. 3.2. 2D sketch of arrangement of PCM and SCB for proposed TES configurations

a) MLSPCM b) SLSPCM-1 c) SLSPCM-2 d) SSCB

3.3 Experimental Setup

Experimental setup consists of stainless-steel (AISI 316) cylindrical energy storage tank of 0.8 m height, 0.381 m outer diameter. Thermal energy storage tank contains multilayers of phase change material encapsulated in the copper tubes and in between the PCM tubes there is cylindrical concrete block. A tank for storage of HTF contains electrical heater of 4KW, heater controller, high temperature pump for the flow of HTF and flow control valve are fitted with the TES tank as shown in Fig.3.3. The high temperature pump is used to reduce the pressure drop across the pipelines. A manual speed controller is attached to pump to vary the mass flow rate for the charging and discharging experiments. The heater controller controls the temperature of HTF and maintains it up to the required limit. Both the tanks are properly insulated by glass wool. The thickness of insulation is 0.0015m. Specifications of TES tank are listed in Table (3.1).

Table 3.1 Specifications of TES tank

Parameters	Value
Height of tank (H_t), (m)	0.8
Diameter of tank (D_t), (m)	0.381
Thickness, (m)	0.01
Porosity	0.65
Aspect Ratio	2.1



Fig. 3.3. Experimental Setup

The experimental setup is further divided into design and fabrication of latent heat storage and sensible heat storage medium.

3.3.1 Latent heat storage medium

D-mannitol and adipic acid are used as phase change materials for the storage of latent heat. PCM's are encapsulated in copper tube with outer diameter of 0.06 m. There are 4 rows of PCM tubes, and each row consist of 3 tubes, placed perpendicular to each other as shown in Fig.3.4.

Top 2 rows of PCM contain D-mannitol at a distance of 0.1016 m from the upper portion and bottom 2 rows contain adipic acid at a distance of 0.1143 m from the bottom of storage tank. To increase the rate of heat transfer between HTF and latent storage and to decrease the charging time copper fins are soldered on each tube. Thermophysical properties of PCM's and dimensions of the PCM tubes are listed in Table (3.2) and (3.3).

Table 3.2 Properties of PCM [1, 2]

Properties	Values	
	D mannitol	Adipic acid
Melting temp (°C)	167	154
Density (kg/m ³)	1520	1360
Specific heat (J/kg K)	1200	1590
Heat of fusion (KJ/kg)	291.47	274.23
Dynamic viscosity (kg/m s)	0.003	0.00454
Thermal conductivity (W/m K)	0.29	0.162
Solidus temp (T _s) (°C)	162.15	149
Liquidus temp (T _l) (°C)	167.8	156

Table 3.3 Specifications of latent section

Parameter	Value
Diameter of tube (D _{PCM}), (m)	0.06
Length of tube (large) (L), (m)	0.28
Length of tube (small) (L), (m)	0.2
Height of PCM rows (H _{PCM}), (m)	0.32
Thickness of tubes (t), (m)	0.04
Diameter of fins (D _f), (m)	0.02
No of fins	384
No of tubes	12



Fig. 3.4. Encapsulated PCM arrangement in rows

3.3.2 Sensible storage medium

Cylindrical concrete block with through holes having outer diameter of 0.35 m and height of 0.25 m is used as sensible storage medium. Holes with the diameter of 0.04 m are designed for the flow of HTF through the sensible storage medium. Properties of sensible storage and specifications of block are presented in Tables (3.4) and (3.5). To increase the retention time and to create the backflow holes are made in the radial direction as shown in Fig.3.5.

Table 3.4 Properties of SCB [3]

Property	Value
Density (kg/m^3)	2750
Specific heat (J/kg K)	916
Conductivity (W/m K)	5

Table 3.5 Specifications of sensible storage section

Parameter	Value
Diameter (D_{SCB}), (m)	0.35
Height (H_{SCB}), (m)	0.250
Holes diameter (D_h), (m)	0.04
No of holes	15



Fig. 3.5. Concrete block with radial and axial holes

3.3.3 Heat transfer fluid

Sunflower oil is utilized as HTF because of its good heat transfer properties and thermal reliability within the medium temperature application. The use of vegetable oils as HTF is increasing for medium and high temperature applications i.e., in domestic and concentrated solar power (CSP) [4, 5]

Charging threshold temperature for HTF is selected to keep the bottom PCM in molten state in order to achieve the effective utilization of tank. Discharging threshold

temperature is the temperature of HTF that is required for certain application. Below this temperature HTF is not acceptable for the application.

Table 3.6 Properties of HTF [6]

Property	Value
Density (kg/m ³)	930.62
Conductivity (W/m K)	0.16
Specific heat (J/kg K)	2115
Viscosity (Pa.sec)	0.0323
Threshold temperature during charging (°C)	160
Threshold temperature during discharging (°C)	120
Temperature at inlet during charging (°C)	190
Temperature at inlet during discharging (°C)	27

Table 3.7 Positions of SCB and PCM for proposed designs

Positions of PCM and SCB	
MLSPCM	PCM-1 at top, PCM-2 at bottom and SCB at the center
SLSPCM-1	PCM-1 at top and SCB at bottom
SLSPCM-2	PCM-2 at top and SCB at bottom
SSCB	Only SCB in the center of tank

3.4 Complete Experimental Procedure

1. During the heat storage phase, the heater controller is set at 190°C to heat the HTF in buffer tank.

2. After heating of HTF up to required temperature the inlet valve of storage tank is opened, and outlet valve is closed for 1st charging cycle.
3. Hot HTF at 190°C is pumped at the top of TES tank at certain mass flow rate. Hot HTF transfer the heat to TES storage mediums (PCM and concrete) and the temperature is recorded using the data logger.
4. After the 1st charging cycle both the inlet and outlet valves are opened and HTF flow in a closed loop and the process of charging continuous until the temperature of storage medium reaches to fluid inlet temperature.
5. During the heat release phase, the connection of heater is removed and cold HTF at temperature of 27°C enters the TES tank from the bottom and gains the heat from storage mediums and flow out from the top. The HTF is discharged directly into the buffer storage tank.
6. After the 1st discharging cycle the HTF flow in closed loop and experimental data is recorded. The process of discharging stops when the temperature of HTF falls below the discharging threshold temperature.

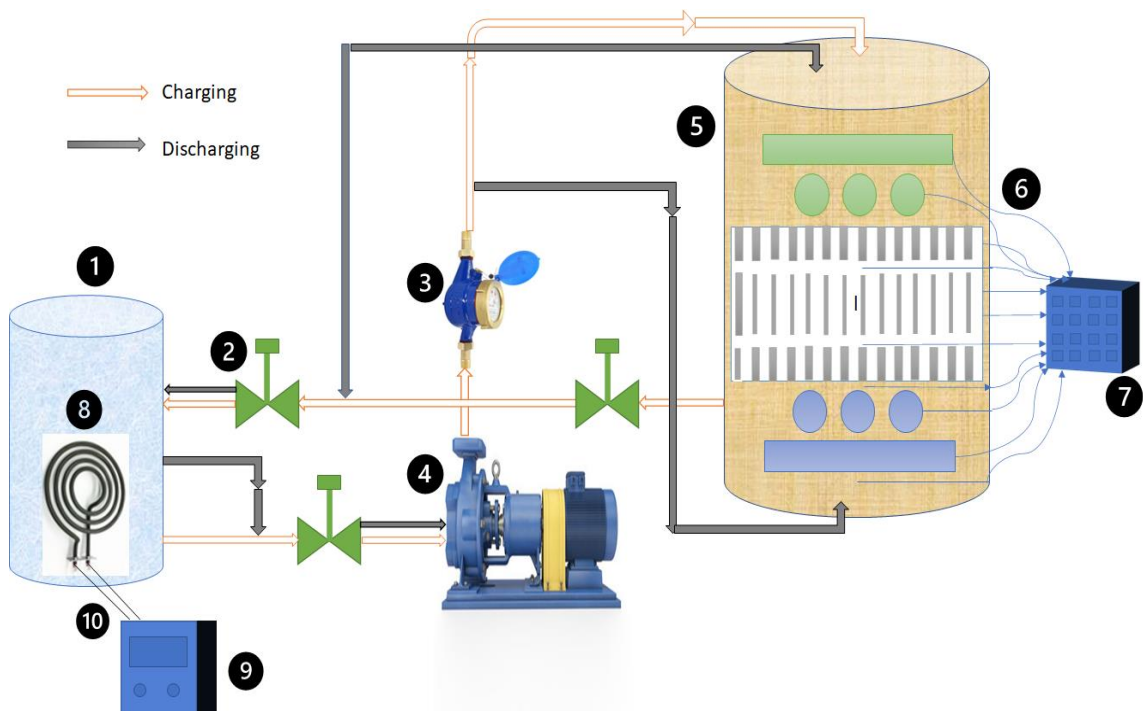


Fig. 3.6. Schematic of experimental setup

1. Buffer tank
2. Flow control valves
3. Flow meter
4. Pump
5. Storage tank with PCM and Concrete
6. Thermocouples
7. Data acquisition
8. Heating rod
9. Heater controller
10. Connecting Wires

3.5 Arrangement of thermocouples in TES and Buffer tank

For SCB, thermocouples are arranged along the axial height of concrete block at different locations (T_s). In latent storage section thermocouples are arranged at the surface of PCM tubes in each row in both radial and axial direction (T_{PCM}). Also, for measurement of HTF temperature in TES tank thermocouples are inserted in radial holes of SCB and space between the bottom PCM tubes and SCB. The temperature at inlet ($T_{inlet, top}$), outlet ($T_{outlet, bottom}$ below bottom PCM) of storage tank and in the buffer storage (T_{HTF}) is also monitored. To measure the temperature of HTF the thermocouples are inserted in the radial holes of concrete block and the space between the block and bottom PCM tubes. The calibration test of thermocouples shows error in temperature measurement is $\pm 0.3C$. Arrangements of thermocouple in TES tank is shown in Fig 3.7.



a)



b)



Fig. 3.7. Storage tank with thermocouples in radial and axial direction a) outer view b) and c) inner view of TES unit

3.6 Thermal performance evaluation

The thermal charging and discharging performance of different design models is discussed based on following set of equations.

3.6.1 Heat energy supplied and removed by HTF

The energy supplied and removed by HTF during charge and discharge process depends upon its inlet and outlet temperatures. Inlet temperature is kept constant in both charging and discharging [7].

$$Q_{\text{sup}} = \dot{m}c_p \int_0^{t_c} (T_{c,\text{in}} - T_{c,\text{out}}) dt \quad (1)$$

$$Q_{\text{sup}} = \dot{m}c_p \int_0^{t_c} (T_{d,\text{out}} - T_{d,\text{in}}) dt \quad (2)$$

3.6.2 Energy gain and recovered by storage medium

Total energy gain and recovered by PCM and SCB depend upon their thermophysical properties and temperature at inlet and outlet portion [8, 9].

$$Q_{g,sen} = \rho_{SCB} V_{SCB} C_{p,SCB} (T_{out} - T_{in}) \quad (3)$$

$$Q_{rec,sen} = \rho_{SCB} V_{SCB} C_{p,SCB} (T_{in} - T_{out}) \quad (4)$$

$$Q_{g,latent} = (\rho_s V_{PCM} C_{p,s} (T_m - T_i)) + \omega \rho_l V_{PCM} L_f + (\rho_l V_{PCM} C_{p,l} (T_{PCM} - T_m)) \quad (5)$$

$$Q_{rec,latent} = (\rho_l V_{PCM} C_{p,l} (T_m - T_i)) + \omega \rho_l V_{PCM} L_f + (\rho_s V_{PCM} C_{p,s} (T_m - T_{PCM})) \quad (6)$$

The total energy for the combined TES storage is the summation of both sensible and latent energy

$$Q_{total} = Q_{sensible} + Q_{PCM} \quad (7)$$

3.6.3 Discharge efficiency

Discharge efficiency of TES is defined as thermal energy recovered by HTF at the end of discharge process to the total stored thermal energy at the end of charging process [10].

$$\eta_d = \frac{\dot{m} C_p \int_0^{t_c} (T_{f,in} - T_{f,out}) dt}{E_{initial}} \quad (8)$$

$$E_{initial} = E_{SCB} + E_{PCM} + E_{HTF} \quad (9)$$

Where,

$$E_{SCB} = \rho_{SCB} V_{SCB} C_p (T_{final} - T_{initial}) \quad (10)$$

$$E_{HTF} = \rho_{HTF} V_{HTF} C_p (T_{final} - T_{initial}) \quad (11)$$

$$E_{PCM} = (\rho_s V_{PCM} C_{p,s} (T_m - T_i)) + \omega \rho_l V_{PCM} L_f + (\rho_l V_{PCM} C_{p,l} (T_{PCM} - T_m)) \quad (12)$$

3.6.4 Charge efficiency

Charge efficiency of TES is the ratio between amount of energy retained by storage medium (SCB and PCM) and total energy supplied by HTF [2].

$$\eta_c = \frac{E_{stored}}{E_{supplied}} \quad (13)$$

3.6.5 Fraction of heat retained by storage medium

The fraction of heat retained by the storage medium (PCM and SCB) is [11]

$$E_{f,PCM} = \frac{Q_{PCM}}{Q_{total}} \quad (14)$$

$$E_{f,SCB} = \frac{Q_{SCB}}{Q_{total}} \quad (15)$$

Where Q_{PCM} and Q_{SCB} are amount of heat retained by PCM and SCB after the discharging time of 80min.

$$Q_{total} = Q_{SCB} + Q_{PCM} + Q_{HTF} \quad (16)$$

3.6.6 Liquid fraction

Liquid fraction is an important parameter which determines the fraction of liquid present in the mixed state (solid and liquid). It ranges between 0 (solid) and 1 (liquid) [12].

$$\omega = \begin{cases} 0 & T < T_s \\ \frac{T - T_s}{T_l - T_s} & T_s < T < T_l \\ 1 & T > T_l \end{cases} \quad (17)$$

3.6.7 Stratification number

Stratification number is the ratio of temperature difference between the axial layers at any time to the maximum temperature difference in TES tank [1].

$$S.N = \frac{(\partial T / \partial y)_t}{(\partial T / \partial y)_{max}} \quad \text{where,} \quad (18)$$

$$(\partial T / \partial y)_t = \frac{1}{Z-1} \left[\sum_{i=1}^{Z-1} \left(\frac{T_i - T_{i+1}}{\Delta y_i} \right) \right]$$

Where,

Z = no of axial layers

T_i = temperature at axial location

T_{i+1} = temperature at adjacent axial location

Δy = distance between the axial layers

Its values range between 0 and 1, with 0 indicates no stratification and 1 means maximum stratification in tank.

3.6.8 Thermocline thickness

Thermal behavior of single tank combined multilayer latent-sensible TES unit is investigated in term of formation and degradation of thermocline thickness profiles. Higher thermocline thickness indicates that TEs have lower discharge efficiency.

$$T_{tc} = \begin{pmatrix} Z(T_{hot}) - Z(T_{cold}) & \text{if } (T_{f,in} \leq T_{hot}) \text{ and } (T_{f,out} \geq T_{tc}) \\ Z(T_{hot}) - 0 & \text{if } (T_{f,in} > T_{cold}) \\ Z - Z(T_{cold}) - 0 & \text{if } (T_{f,out} < T_{hot}) \end{pmatrix} \quad (19)$$

Where, Z represents axial height of block and T_{cold} and T_{hot} in present study are 35°C and 190°C, respectively.

Summary

In this chapter detailed experimental procedure is discussed. Complete description of all the components used in storage unit followed by mathematical equations required for thermal performance evaluation of TES are presented. This section includes the detail of different TES designs proposed for certain applications. Specifications of storage medium (PCM and SCB), storage tank and tank for storage of HTF (buffer tank) are also discussed.

References

1. Mawire, Ashmore Ekwomadu, Chidiebere S Shobo, and Adedamola B., Experimental charging characteristics of medium-temperature cascaded packed bed latent heat storage systems. 2021. **42**: p. 103067.
2. Ahmed, N Elfeky, Ke Lu, Lin Wang, QW., Thermal performance analysis of thermocline combined sensible-latent heat storage system using cascaded-layered PCM designs for medium temperature applications. 2020. **152**: p. 684-697.
3. Wu, Ming Li, Mingjia He, Yaling Tao, Wenquan., Thermal Performance of High Temperature Concrete Thermal Storage System for Solar Thermal Power Generation. 2013. **47**(5).
4. Mawire, Ashmore Phori, Abigail Taole, and Siemon., Performance comparison of thermal energy storage oils for solar cookers during charging. 2014. **73**(1): p. 1323-1331.
5. Hoffmann, J.-F Vaitilingom, Gilles Henry, J-F Chirtoc, M Olives, R Goetz, V Py, X., Temperature dependence of thermophysical and rheological properties of seven vegetable oils in view of their use as heat transfer fluids in concentrated solar plants. 2018. **178**: p. 129-138.
6. Mawire, Ashmore., Performance of Sunflower Oil as a sensible heat storage medium for domestic applications. 2016. **5**: p. 1-9.
7. Li, Meng-Jie Qiu, Yu Li, and Ming-Jia., Cyclic thermal performance analysis of a traditional Single-Layered and of a novel Multi-Layered Packed-Bed molten salt Thermocline Tank. 2018. **118**: p. 565-578.
8. Niyas, Hakeem Rao, and Chilaka Ravi Chandra Muthukumar., Performance investigation of a lab-scale latent heat storage prototype—experimental results. 2017. **155**: p. 971-984.
9. Rao, Chilaka Ravi Chandra Niyas, and Hakeem Muthukumar., Performance tests on lab-scale sensible heat storage prototypes. 2018. **129**: p. 953-967.

10. Ahmed, N Elfeky, Ke Lu, Lin Wang QW., Numerical characterization of thermocline behaviour of combined sensible-latent heat storage tank using brick manganese rod structure impregnated with PCM capsules. 2019. **180**: p. 243-256.
11. Zanganeh, Giw Commerford, Mark Haselbacher, Andreas Pedretti, Andrea Steinfeld, Aldo., Stabilization of the outflow temperature of a packed-bed thermal energy storage by combining rocks with phase change materials. 2014. **70**(1): p. 316-320.
12. Bashirpour-Bonab, Hadi., Investigation and optimization of PCM melting with nanoparticle in a multi-tube thermal energy storage system. 2021. **28**: p. 101643.

Chapter 4

Results & Discussions

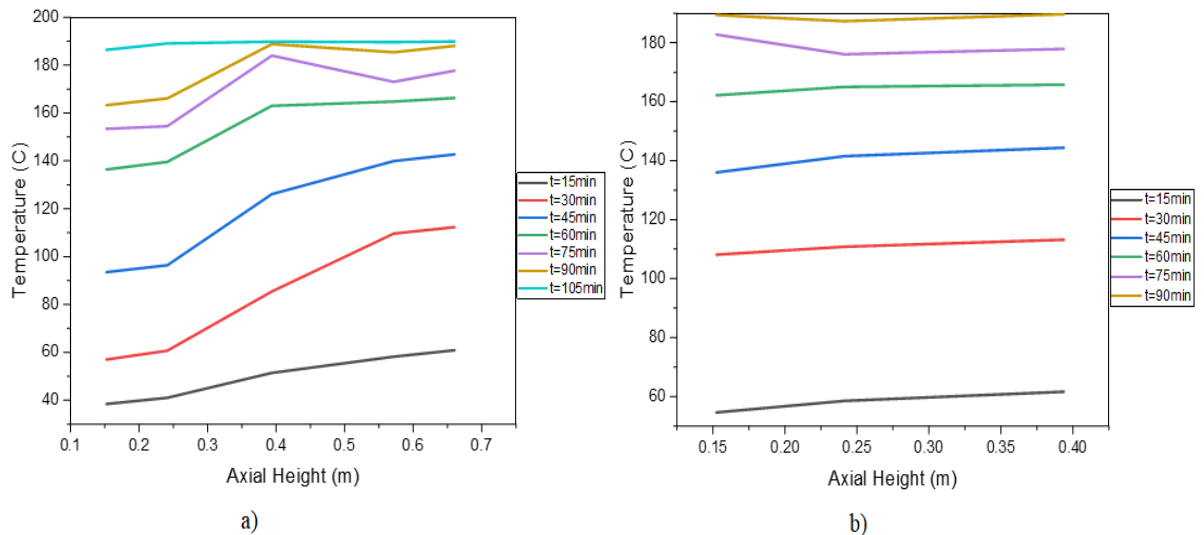
4.1 Thermal performance of TES systems

In the present model of combined multilayer TES system, the melting points of PCM are chosen intelligently i.e., PCM at top is of high and bottom PCM have low melting temperature. This arrangement of storage medium enhances the charging and discharging time and helps to store and extract maximum thermal energy. The threshold temperature for discharging is set at 120°C and this is the temperature required for certain medium temperature application. Similarly, for the charging process the maximum limit of temperature is 160°C. This temperature is to keep the bottom PCM in molten state to achieve the effective utilization of TES system.

4.1.1 Thermocline temperature profiles

Thermal performance of single TES unit is predicted by thermocline thickness. The lower the thickness effective will be charge and discharge performance. To predict the thermocline behavior temperatures of HTF at different heights along axial direction are plotted in Fig.4.1. During the charge process in Fig. 4.1(a, b, c, d) hot fluid enters at the top and exchanges the heat with the storage medium. After $t=45\text{min}$ for SLSPCM-2 the PCM-2 at the top is completely in molten state while the portion of PCM capsules at the top of SLSPCM-1 and MLSPCM are still in phase transition phase. Simultaneously, after the charging period of 75min the melting of entire PCM's at the top of SLSPCM-2 and MLSPCM occurs. After these instants hot HTF propagates with high velocity through the tank. This is because high melting PCM-1 (162.15°C) at the top for SLSPCM-2 and MLSPCM takes longer time for changing its phase while the melting temperature of PCM-2 at the top of SLSPCM-1 is low (151°C) which results in quick propagation of hot region downward. Moreover, for low melting point PCM the temperature difference between hot HTF and PCM melting point is high which increases the rate of heat transfer. As a result of this quick degradation of thermocline layer occur in SLSPCM-1 as

compared to other configurations. It can be clearly seen that less thermal gradient or thermocline exist between the different layers at different heights for SSCB. This is because structure doesn't have any layers of different melting temperatures. Therefore, the thermocline thickness for the SSCB is more as compared to combined latent-sensible heat configurations. It is observed that the propagation of hot region from top is same for SLSPCM-2 and MLSPCM. The reason is that both configurations have same melting point PCM with the same volume fraction. Moreover, after charging time of 60 min for MLSPCM, SLSPCM-1 and almost 50min for SLSPCM-2, respectively, the change in trend of HTF is observed for all three configurations because temperature of PCM 1 at top remain constant for some time while SCB stores only sensible heat, and its temperature increases continuously. It is also because SCB have high thermal conductivity, it gains the heat quickly as compared to PCM.



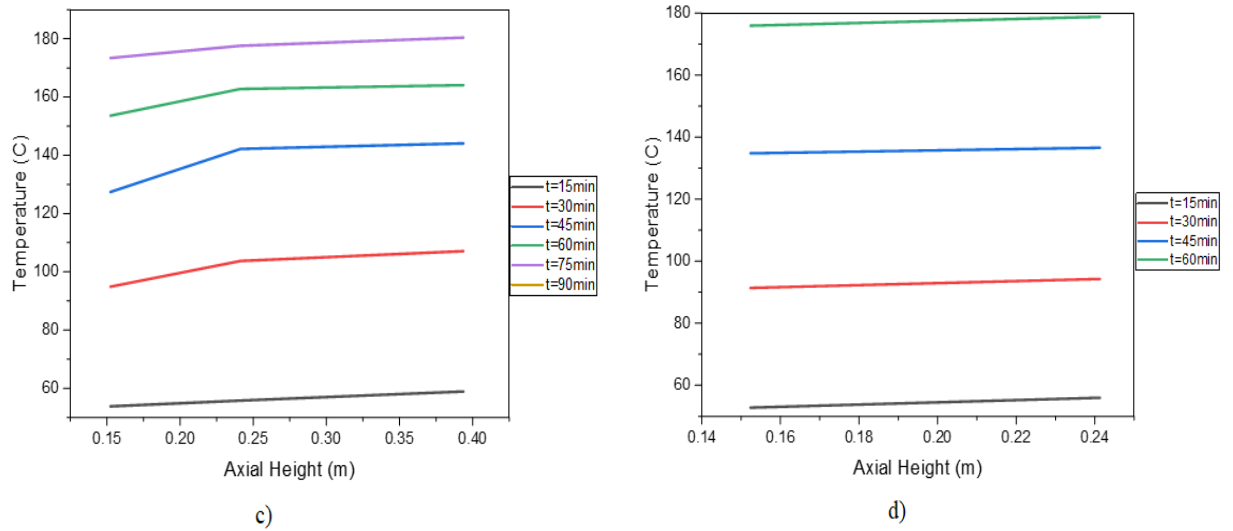


Fig. 4.1. Distribution of temperature profiles along axial height of tank a) MLSPCM b) SLSPCM-1 c) SLSPCM-2 d) SSCB during charging

Fig. 4.2 (a, b, c, d) shows fluid temperature profiles during discharging. Low solidification point PCM at the bottom effectively enhance discharging performance of energy storage system. Because it doesn't allow the rapid propagation of cold region upward and thus limiting the rapid increase in thermocline thickness. The comparative results show that completion of solidification process of MLSPCM takes more time compared to SLSPCM-2, SLSPCM-1 and SSCB respectively. It is observed that for MLSPCM the low temperature PCM 2 at bottom reaches to its phase transition temperature of 152°C after discharging period of 35 min, while at the same time temperature of PCM 1 at top is about 170°C which indicates that it is still releasing its sensible heat. The PCM at top starts releasing the latent heat almost 15 min after the PCM 2 which increases the discharging time. While SLSPCM-2 and SLSPCM-1 both have sensible storage medium at the bottom which discharges quickly as compared to PCM. The results show that effective discharge time of SLSPCM-1 is 55min which is less compared to SLSPCM-2 because it has high solidification temperature PCM at the top of concrete block which solidifies quickly. From the temperature profile of SSCB it is noticed that at t=30min the temperature of SCB is 119.1°C (effective discharge temperature) concrete block at releases its store sensible heat rapidly which result in quick degradation of thermocline layer. In Fig.4.2,

in all the designs the temperature at the center drops more as compared to top and bottom. This is because temperature is measured at the surface and surface contact in case of SCB with HTF is more and heat dissipation is more. Also, the holes in the radial direction in concrete block creates the back flow and turbulence of HTF which increases the retention time and increases the heat transfer. Therefore, these findings reveal that proposed combined multilayer latent-sensible storage design performs consistently during both charging and discharging.

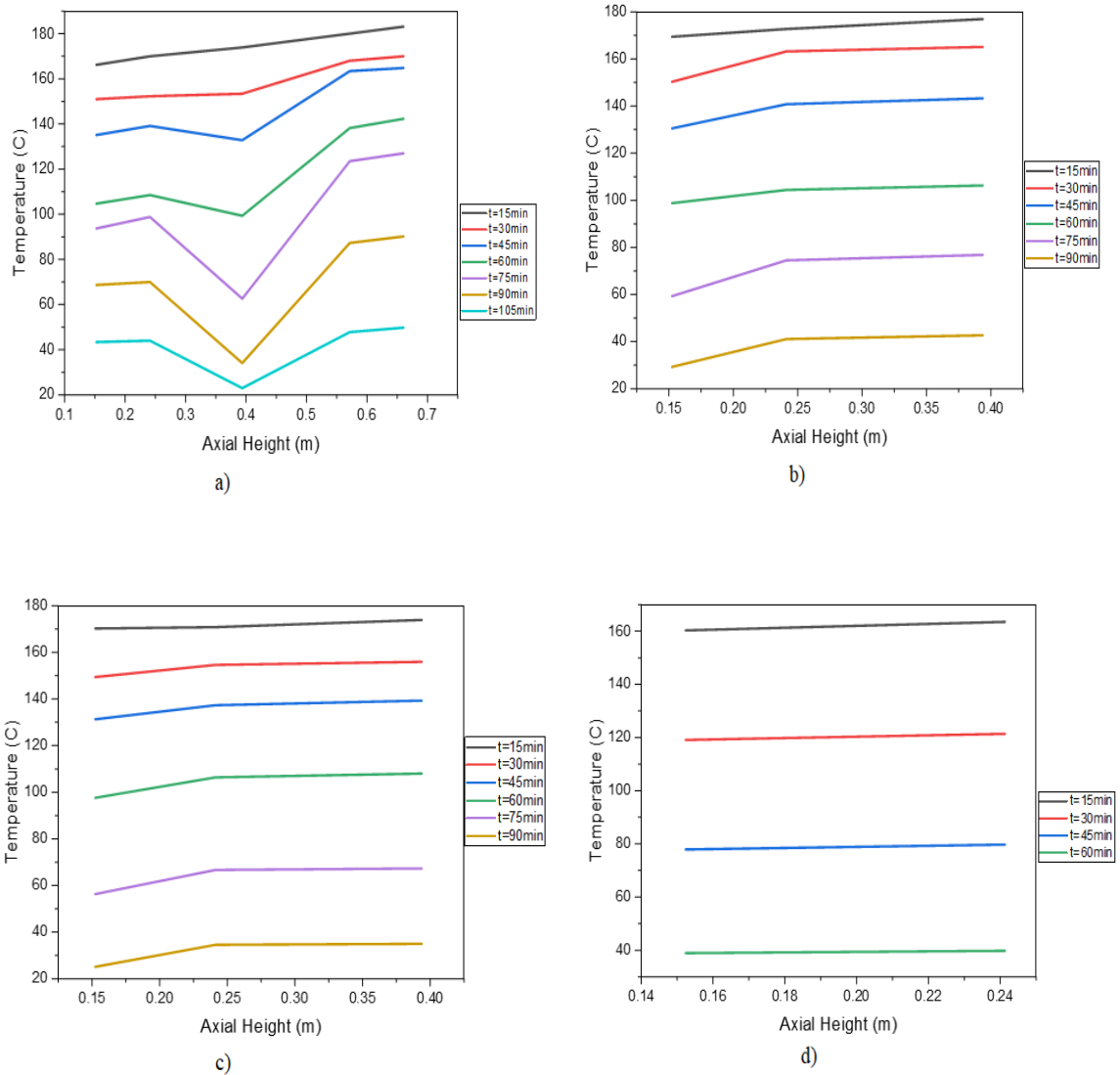


Fig. 4.2. Distribution of temperature profiles along axial height of tank for a) MLSPCM b) SLSPCM-1 c) SLSPCM-2 d) SSCB during discharging

4.1.2 Temperature profile of fluid at center

Fig.4.3 indicates the comparative fluid temperature profiles w.r.t time at center ($x = H/2$) for MLSPCM, SLSPCM-1, SLSPCM-2 and SSCB, respectively during charging and discharging. It is noticed that for SLSPCM-2 at charging time of $t=30\text{min}$ temperature of fluid is 94.9°C while fluid at the center for MLSPCM is at 85.4°C . The results indicates that temperature of fluid for SLSPCM-2 is at higher values compared to MLSPCM and SLSPCM-1. This is due to presence of same volume of low melting temperature PCM at the upper part, high exergy fluid moves rapidly in downward direction. While MLSPCM and SLSPCM-2 contain same volume of high temperature PCM at inlet, which results in low exergy fluid flow for the incoming storage medium in the tank for the longer period. In SSCB the temperature at the center increases quickly compared to other TES configurations. It reaches to the temperature of 136.6°C after the charging time of 45min . This is because of increase in heat transfer between HTF and concrete. Also due to lack of either high or low melting temperature PCM there is no hindrance for the flow of high energy fluid along axial direction.

During discharging the HTF temperature profile of MLSPCM shows better thermocline performance. It means temperatures at the center are at higher values compared to other designs. This is because of low solidification temperature of PCM at the bottom releases its stored thermal energy for the longer period and limits the rapid movement of cold fluid upward. takes the advantage of incoming HTF. This enhances the extraction of maximum stored latent and sensible energy. While for SLSPCM-1 and SLSPCM-2 temperature at the center drops rapidly due to quick heat release by the sensible storage at the bottom. The graph shows that temperature of fluid at $t=75\text{min}$ for MLSPCM is 62.6°C followed by 59.3°C , 56.3°C for SLSPCM-1 and SLSPCM-2, respectively. While for SSCB the temperature at the centers drops quickly i.e., for $t=55\text{min}$ it reaches at the temperature of 51.7°C means cold region moves upward quickly which results in worst thermocline performance.

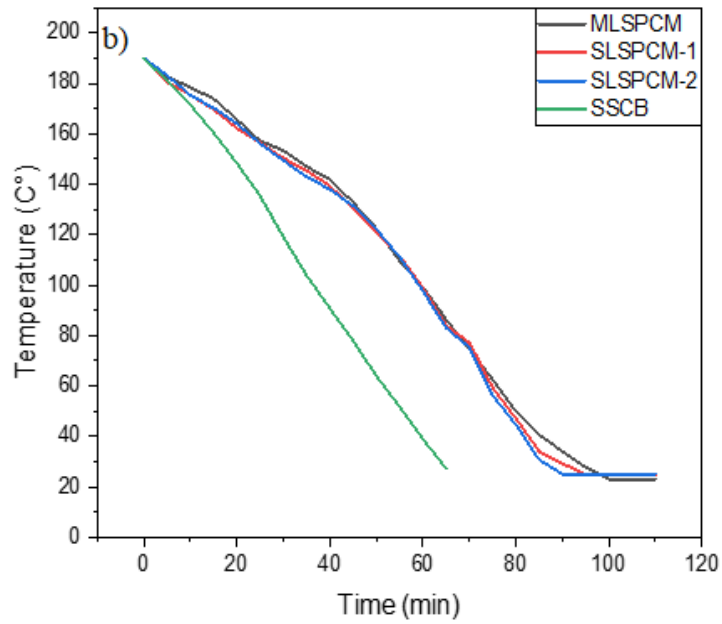
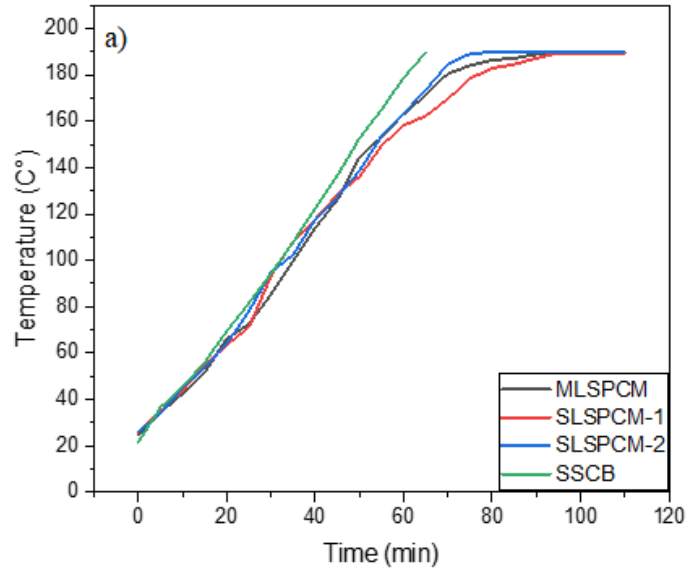


Fig. 4.3. Comparative fluid temperature profile at $x=H/2$ for four configurations

a) charging b) discharging

4.1.3 Comparative temperature profiles of PCM, SCB and HTF

The comparative temperature profiles of PCM, SCB and HTF for charging and discharging process are shown in Figs. 4.4 and 4.5. During charging the temperature of HTF is at higher value as compared to storage medium (SCB and PCM). Fig. 4.4(a) shows that for MLSPCM, SLSPCM-1 and SLSPCM-2, respectively the temperature difference at the beginning of charge process is high because the conduction of heat is less but as PCM-1 and PCM-2 gains the heat the temperature difference between HTF and PCM's decreases become almost zero after the phase transition state. It is also noticed that HTF close to PCM-1 and PCM-2 also show the constant temperature profile close to melting temperature of PCM's. The results show that temperature difference between HTF and PCM at the top decreases quickly for SLSPCM-2. It is clear from the temperature profiles that at the charging time of almost 45min HTF is at 141.8°C while PCM-2 is at temperature of 144.1°C. This is because PCM at the top reaches to its phase transition state abruptly due to greater heat driving force. Similarly, during the initial charging cycle for all the TES designs in Fig. 4.4(b) the temperature difference between SCB and HTF is more because transfer of heat from HTF to concrete block is less. But as the charging process continuous SCB starts storing sensible heat, its temperature increases and the difference of temperature decreases. The comparative temperature profiles indicates that at t=45min temperature of SCB and HTF for MLSPCM are 121.7°C and 126.1°C followed by 128.4°C, 135.4°C, 126.7°C, 127.4°C, and 135.5°C, 136.6°C for SLSPCM-1, SLSPCM-2 and SSCB respectively. It is seen that for SLSPCM-2 the high exergy HTF moves swiftly along the axial height of tank which decreases the temperature difference in less time compared to other combined sensible-latent TES designs. For SSCB the temperature difference between SCB and HTF decreases rapidly because of quick heat transfer by fluid. It is also observed that temperature difference between SCB and HTF decreases rapidly as compared to temperature difference between PCM's and HTF. This is because sensible storage gain temperature quickly as compared to PCM. From the results it is seen that initially the thermocline thickness for MLSPCM is low but as soon as the storage medium start gaining heat the temperature gradient between the top and bottom of TES tank decreases and thermocline thickness increases. The thermocline thickness for

MLSPCM system is low over a large charging time which increased the storage capacity of system.

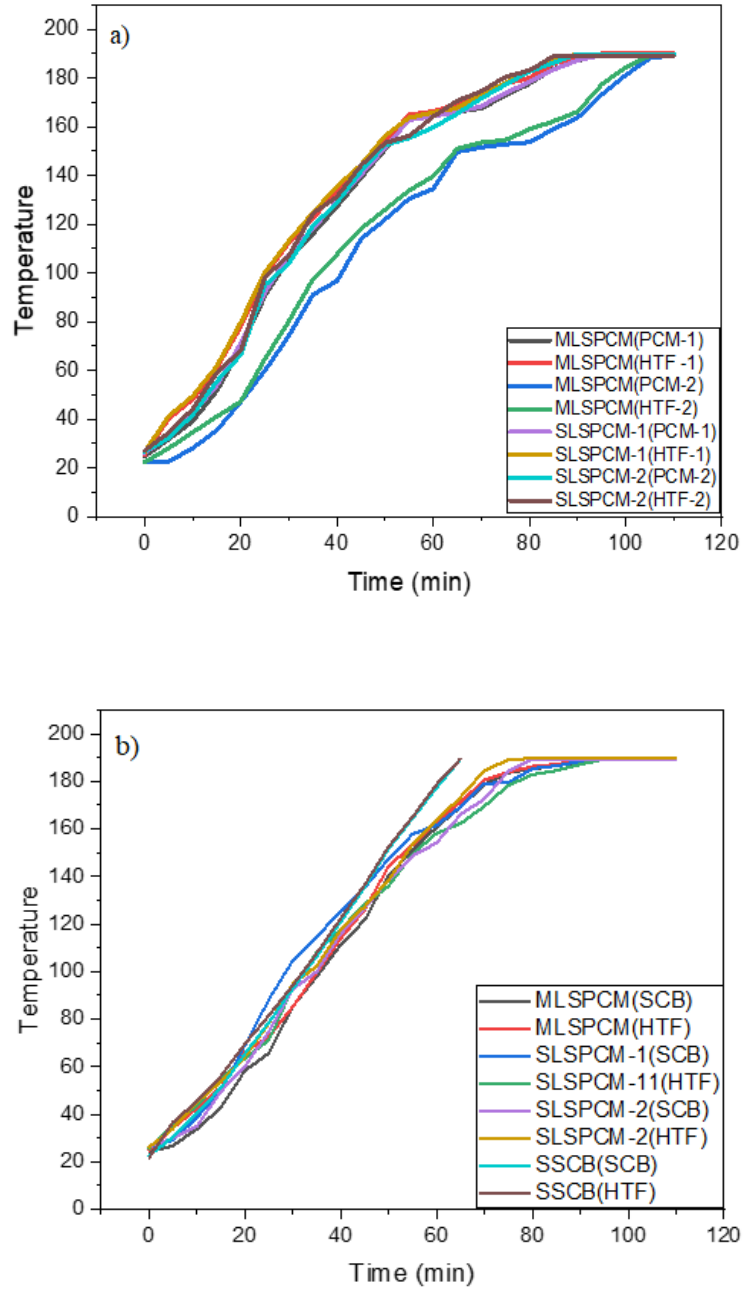


Fig. 4.4. a) Comparative temperature profile of PCM and HTF b) Comparative temperature profile of SCB and HTF for four configurations during charging

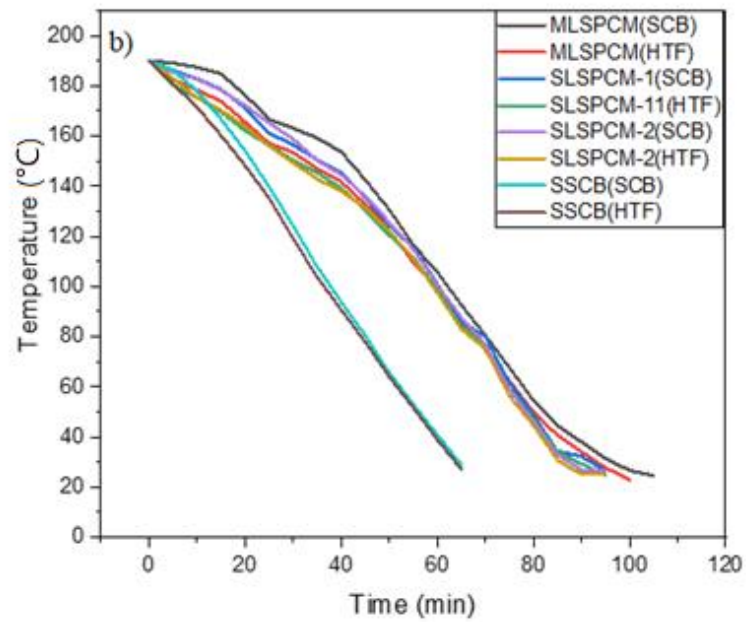
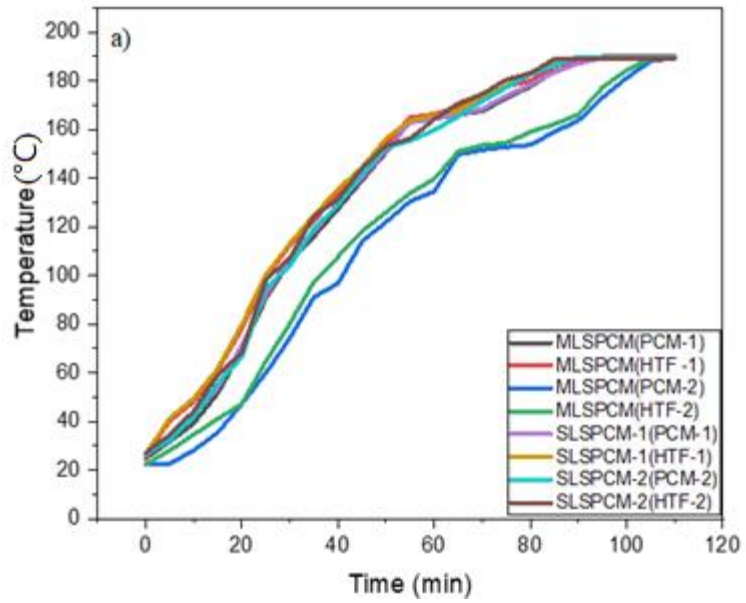


Fig. 4.5. a) Comparative temperature profile of PCM and HTF b) Comparative temperature profile of SCB and HTF for four configurations during discharging

Fig.4.5 shows that during discharging temperature of HTF is at lower value as compared to top and bottom PCM and concrete block. The results indicate that for MLSPCM, SLSPCM-1 and SLSPCM-2 the temperature of HTF close to PCM-1 and PCM-2 decreases quickly until PCM's reach to their melting temperatures. But as the PCM releases stored heat the temperature difference decreases and becomes small after the phase transition. Temperature profiles of HTF show that there is very slight reduction of temperature as long as PCM releases its latent heat. The comparative temperatures of HTF and PCM at the top section for MLSPCM at discharging time of 60min are 138.2°C, 143.8°C followed by 104.4°C, 106.2°C and 106.4°C, 109.7°C for SLSPCM-1 and SLSPCM-2, respectively. For SLSPCM-1 temperature of HTF at the top section reduces quickly compared to SLSPCM-2 because of quick solidification of PCM. While for MLSPCM the temperature of HTF at top section is still at higher value because the low solidification temperature PCM at bottom limits the movement of cold region in upward direction. The temperature distribution curves for combined sensible-latent heat TES system indicates that the temperature of HTF at outlet section remains constant for some period because the PCM placed near the outlet creates thermal buffer effect. This effect is maximum for MLSPCM which make use of both the high and low solidification temperature PCM and supply HTF at constant temperature for more time which enhances the effective utilization of stored energy. While the temperature history of the sensible storage shows that as the time passes it losses sensible heat and its temperature start decreasing. So, temperature of HTF also start decreasing after some time because it will not acquire enough heat from sensible storage. Due to this effect SSCB discharges quickly compared to MLSPCM, SLSPCM-1 and SLSPCM-2, respectively.

4.1.4 Stratification number

Stratification in the TES tank is explained using the dimensionless number as shown in Fig.4.6. During the start of charging process maximum heat transfer occurs at the top section of tank while the temperature at the bottom portion is still low. Thus, more temperature gradient exist across the height of storage tank until the temperature at outlet starts increasing. The graph indicates that MLSPCM takes more time to achieve the maximum value of stratification number. This is due to higher melting temperature

medium (D-mannitol) at the top the hot region propagates slowly in downward direction and the temperature at bottom of tank is increasing gradually. MLSPCM achieve its maximum value almost at the charging time of 60 min. While SLSPCM-2 attain the peak stratification number quickly. This is because in SLSPCM-2 the PCM at the inlet melts quickly which result in decrease in the thermal gradient between the different heights. In case of SSCB, concrete block stores the sensible heat rapidly because to its high conductivity and achieve the maximum stratification in shortest time compared to all designs. The charging time at which SLSPCM-2 and SSCB reaches to its maximum value are 40min and 20min respectively. The maximum value of stratification number for MLSPCM is 0.999277 followed by SLSPCM-1, SLSPCM-2 and SSCB having values of 0.958661, 0.992806, 0.842435 respectively. It is noticed that SLSPCM-1 and MLSPCM the thermal gradient is maximum and maintained for longer period compared to SLSPCM-1, although both have same melting temperature PCM at the top. This is because MLSPCM takes the advantage of both high and low melting temperature PCM's.

Decline of stratification number is observed in all the configurations as the temperature at the bottom of tank increases. The decline of stratification number for MLSPCM, SLSPCM-1, SLSPCM-2 and SSCB occurs after the charging time of almost 60min, 50min, 35min and 25min respectively. The slight jump appears in stratification curve of MLSPCM after 70 min, this is because the PCM at the bottom is melting and change in temperature is less, while the temperature at the upper of tank is increasing continuously. While no jump occurs in SLSPCM-1, SLSPCM-2 and SSCB because these arrangements have no PCM at the bottom section.

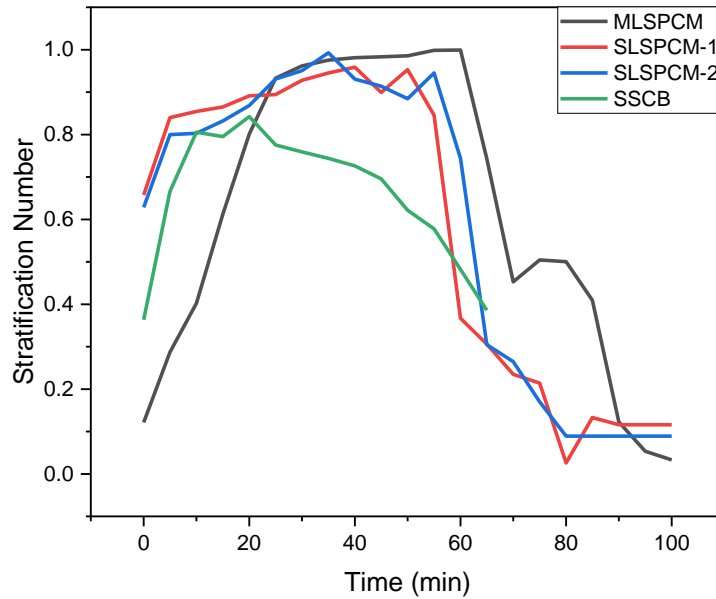


Fig. 4.6. Stratification number for proposed TES designs w.r.t time

4.1.5 Comparative temperature profile of fluid at outlet section

The comparison of fluid temperature at the outlet as a function of time for the proposed four configurations during charging and discharging is shown in Fig.4.7. During the charge process in Fig. 4.7(a) the hot fluid enters from the top and exchange heat with storage medium. The results show that the slope of curve for MLSPCM is gentle which enhance the charging time but using the multilayer PCM with increase in melting point downward and high heat of fusion PCM at the top increases its storage capacity. The high heat of fusion help to enhance the charging time of storage tank. The outlet temperature profiles for SLSPCM-1, SLSPCM-2 and SSCB have steeper slope which exhibits that these arrangements of storage medium take less time to charge. It is noticed that in SLSPCM-2 the hot HTF moves quickly along the height of tank because of rapid melting of PCM at the inlet portion which reduces its charging time. SLSPCM-1 and MLSPCM both have same PCM at the top but for SLSPCM-1 the charging time is reduced due to single layer of PCM. Also, the energy storage capacity of SLSPCM-2 is more compared to SLSPCM-1. The temperature profiles indicate that SSCB takes 26.3%, 31.5% and

40.9% less time to charge compared to SLSPCM-1, SLSPCM-2 and MLSPCM respectively. Because there is no hindrance for hot HTF due to lack of both high and low melting temperature PCM. Fig.4.7 (b) shows that MSPCM and SSCB have the satisfactory and unsatisfactory worst discharging performance. During discharge process, for all the design configurations except SSCB initially the temperature of HTF at outlet is not decreasing quickly. This is because thermocline thickness expands steadily at the start. As soon the cold region moves upward the temperature of HTF drops and show the phase transition close to melting temperature of top PCM. Then the fluid starts releasing the sensible heat and temperature reaches to minimum. MLSPCM has highest discharge time of 105min followed by SLSPCM-2, SLSPCM-1, SSCB with 95min, 90min and 65min respectively. This show that using the multilayer PCM with different solidification temperatures along with sensible storage enhance the extraction of stored energy. Discharging time for SLSPCM-2 is more than SLSPCM-1 because of low solidification point PCM at the outlet which takes time to solidify although the concrete block in both the configurations is discharged quickly. The graph indicates that PCM placed near the outlet section of MLSPCM, SLSPCM-1 and SLSPCM-2 respectively, remain in molten state and maintain constant temperature of outgoing HTF during discharging. The temperature of outgoing HTF is stabilize for some time which increase the discharge time and efficiency. In MLSPCM stabilization of temperature occurs for more time which enhances its utilization ratio and discharge efficiency. In SSCB the temperature at the outlet section is decreasing continuously because of only sensible heat releases by the storage medium. It is also noticed that because of irregular heat transfer along the radial direction, the PCM at the sides solidify quickly compared to material in the center. As a result of this some part of heat is trapped in PCM and remain unused.

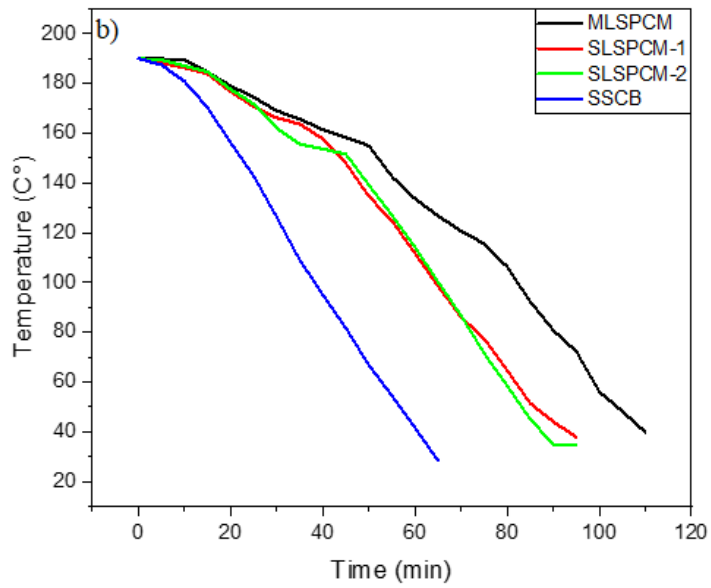
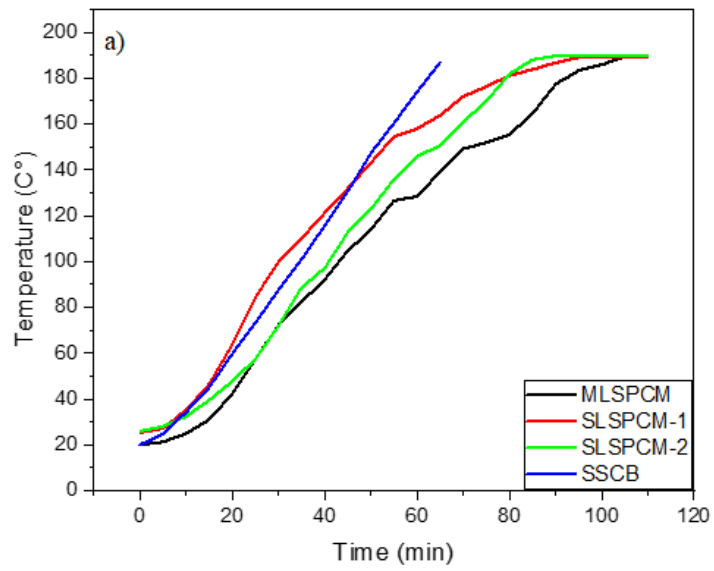


Fig. 4.7. Temperature of fluid w.r.t time at outlet section a) during charge b) discharge process

4.1.6 Variation in liquid fraction

Fig.4.8 shows the change in liquid fraction w.r.t time during charge and discharge process for different design configurations. During charging, for MLSPCM the liquid fraction is 0 until the period of 50min for both the PCM's, as they are in solid phase and storing only sensible heat. As the process continuous and the fluid exchanges the heat with the storage material the percentage of liquid increases. During the phase transition state, the liquid fraction is in between 0 and 1 which indicates the presence of both liquid and solid states. The results shows that PCM 1 at top starts melting after charging time of 55 min while the PCM 2 at the bottom is still storing the sensible heat. This is due to the higher heat transfer potential available at the inlet of tank. It is noticed that liquid fraction for SLSPCM-2 changes rapidly after $t=45\text{min}$ because of low melting temperature PCM 2 while, for MLSPCM and SLSPCM-1 liquid fraction at the top changes almost at the same time. It took about 80min, 70min, 55min to attain the molten fraction of unity for MLSPCM, SLSPCM-1 and SLSPCM-2 respectively. During discharge process, the storage medium (PCM) releases its stored heat, and the liquid part decreases with the time. For MLSPCM, the liquid fraction PCM 2 at bottom decreases after the discharge period of 25 min while for PCM 1 at top the liquid fraction is still unity. Within this period the PCM 1 is releasing its stored sensible heat. This is because during discharging the cold fluid enters from the bottom of tank and it exchanges the heat firstly with the PCM at the bottom. It took about 45min, 35min, 40min for MLSPCM, SLSPCM-1, SLSPCM-2 respectively, to reach the molten fraction of zero. It is noticed that for SLSPCM-2 the PCM 2 takes more time to release its latent heat compared to SLSPCM-1 because of its low solidification temperature and it enhances the discharging also.

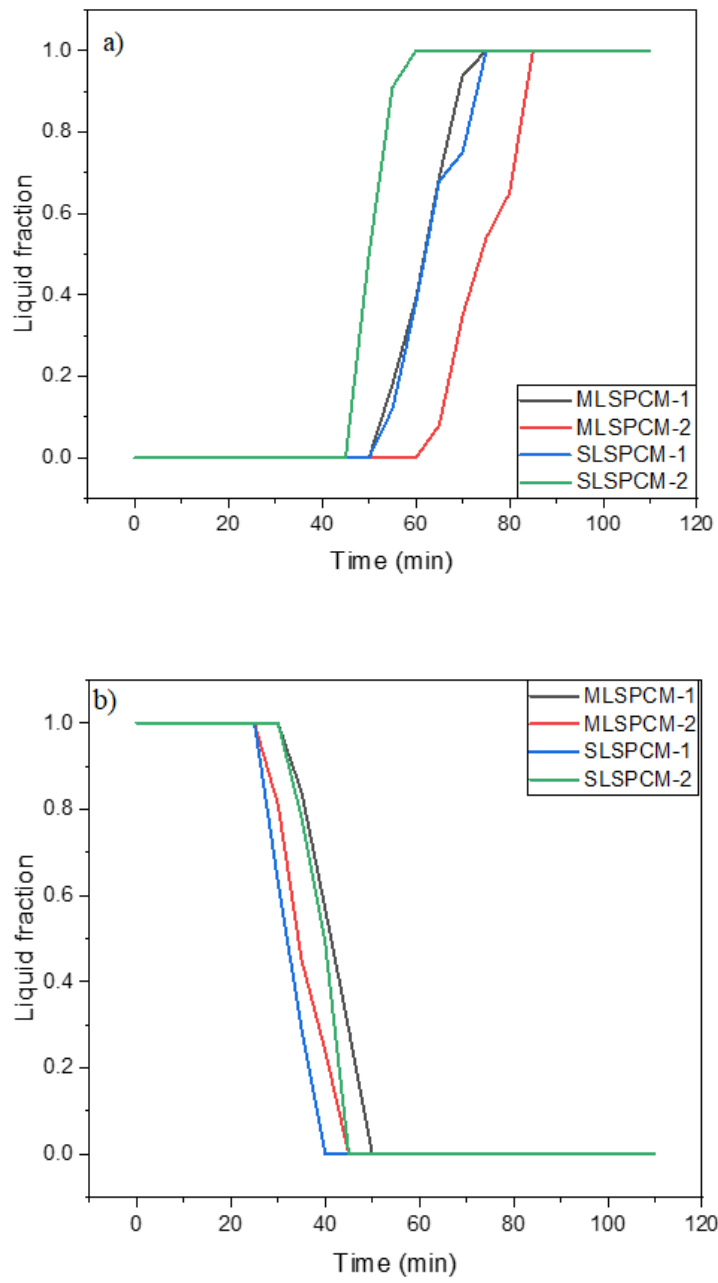


Fig. 4.8. Variation of liquid fraction of PCM's with time a) charge b) discharge process

4.2 Performance parameters for proposed TES systems

4.2.1 Thermal energy transferred and removed by HTF

The thermal energy transferred during the charge for different TES configurations is shown in Fig.4.9 (a). The effective energy supplied by HTF depends upon threshold temperature (160°C). The graph indicates that MLSPCM show the best performance compared to other the other configurations and achieves a maximum value of 13.9kWhr at the end of charging period followed by 11.49kWhr, 10.71kWhr and 4.55kWhr for SLSPCM-1, SLSPCM-2 and SSCB, respectively. This is because of high storage capacity of PCM 1 at the inlet. SSCB show the reduced thermal performance because of high heat transfer between HTF and sensible storage which reduces its charging time. It is noticed that MLSPCM show better performance compared to SLSPCM-1 because of combination of high and low melting point PCM's in single tank. Fig. 4.9(b) depicts the comparative energy extraction profile during discharge process. The thermal energy removed by HTF from the storage medium depends upon the threshold temperature (120°C). MLSPCM show grater energy extraction value of 12.44kWhr followed by 10.11kWhr, 10.25kWhr and 3.88kWhr for SLSPCM-1, SLSPCM-2 and SSCB, respectively. It is seen that due to presence of low solidification temperature PCM-2 at the top of concrete block enhances the charging time of SLSPCM-2 (about 5-10min) therefore, HTF extracts more stored energy than SLSPCM-1. SSCB discharges quickly after 65min. Whereas, SLSPCM-1 and SLSPCM-2 are still delivering the useful stored energy. Whereas MLSPCM show highest discharging time of 110min which results in extraction of more stored energy than all the proposed configurations. Moreover, it is noticed that the PCM at the outlet section creates thermal buffering effect which also enhance the discharging time for combined latent-sensible storage designs and more energy is extracted. The results indicates that multilayered PCM with proper melting and solidification temperature enhances the energy storage and extraction capacity.

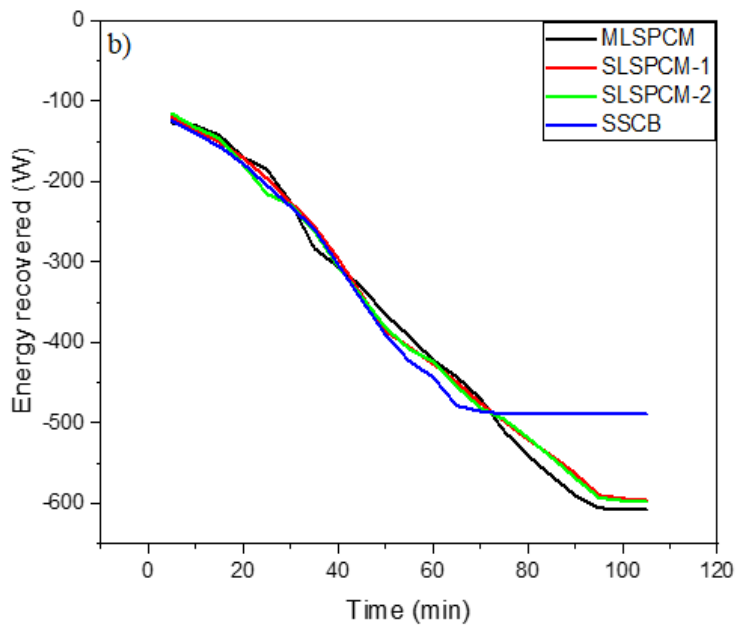
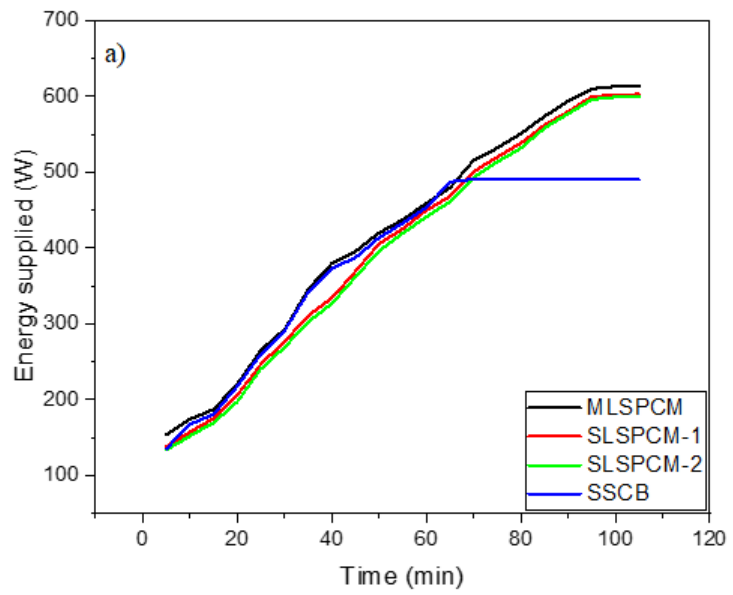


Fig. 4.9. Thermal energy a) supplied during charge b) removed by HTF during discharge process

4.2.2 Thermal energy accumulated and retrieved by storage medium

Fig. 4.10(a and b) indicates the amount of thermal energy accumulated and retrieved by the storage medium. The comparative results show that MLSPCM attain the highest energy storage value of 45116.72kJ followed by 38769.03kJ, 37167.2kJ and 31991.57kJ for SLSPCM-1, SLSPCM-2 and SSCB, respectively. The slow movement of hot HTF along the height of tank due to high melting PCM-1 at the top increases the storage capacity of MLSPCM. Moreover, multilayers of PCM stores more than half of the total stored energy in MLSPCM configuration. The amount of energy stored by PCM in MLSPCM, SLSPCM-1, SLSPCM-2 are 24206.56kJ, 13475.17kJ and 11927.1 kJ, respectively. Moreover, it is noticed that SSCB exhibits less storage capacity compared to other proposed designs. This is due to presence of only sensible storage medium energy. SLSPCM-2 stores less energy during charging compared to SLSPCM-1 because of low melting temperature PCM the charging time is reduced and as a result of this PCM stores less energy. During discharge process the amount of energy removed from the storage medium for MLSPCM is high having value of 40378.29kJ followed by 31639.94kJ, 32050.069kJ and 31385kJ for SLSPCM-1, SLSPCM-2 and SSCB, respectively. This is because PCM 2 at bottom requires more time to achieve its low solidification temperature which restricts the movement of cold region in upward direction, and this enhances the extraction of stored energy. SLSPCM-2 extracts more energy compared to SLSPCM-1 because it is discharged for more period due to low solidification temp of PCM, although both have same volume of PCM at the top portion. SSCB delivers the energy for shorter period because of release of only sensible heat. Also, the losses from the tank are more because volume of storage medium in the tank is less which reduces the ability to extract the stored energy. From these results it is concluded that combining the multilayered PCM concept with combined sensible-latent TES configuration increases the energy storage and energy extraction from the storage medium.

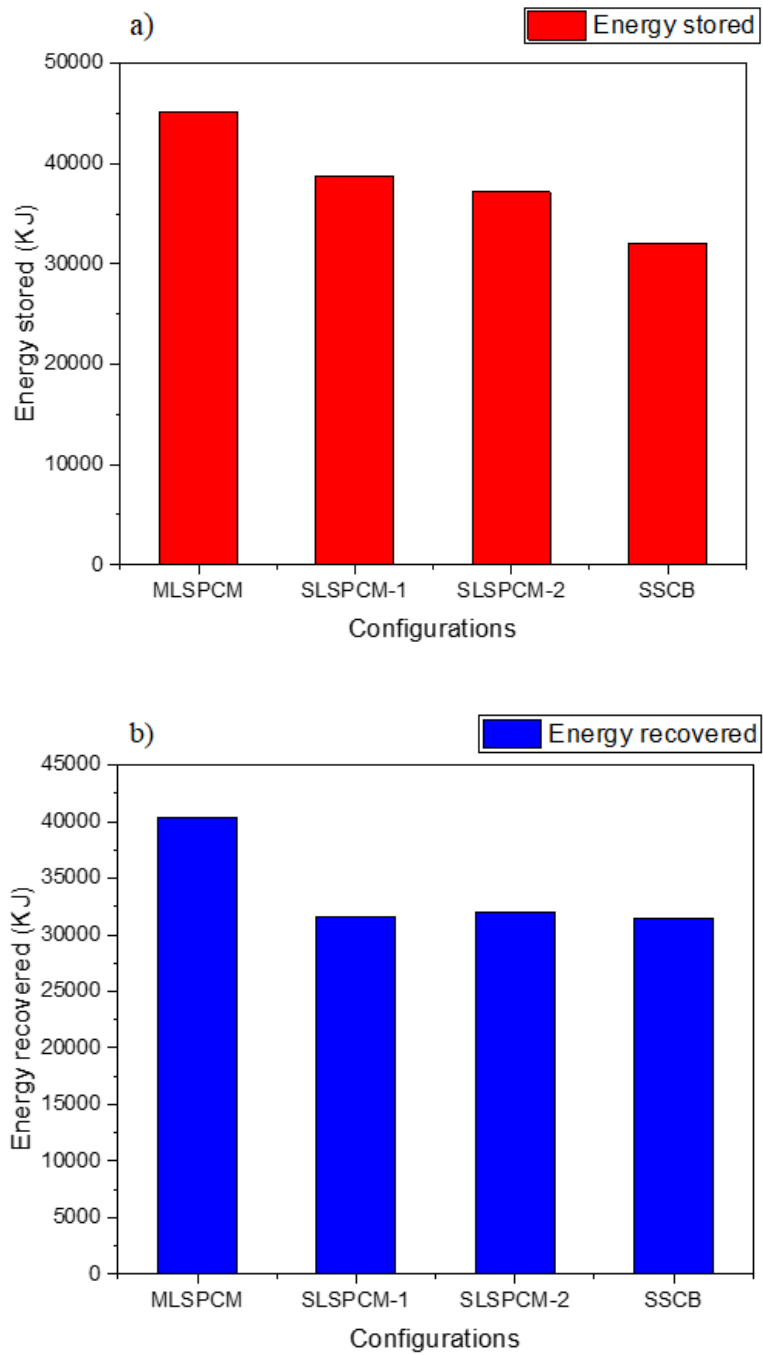


Fig. 4.10. Total energy a) stored by storage medium during charge b) recovered during discharge process for proposed TES designs

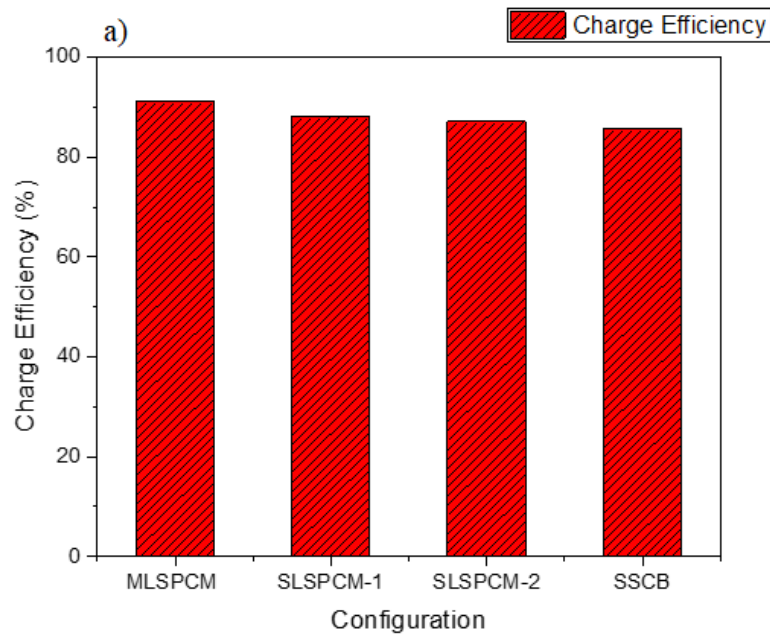
Table 4.1 Performance parameters for four configurations

Performance Parameters	MLSPCM	SLSPCM-1	SLSPCM-2	SSCB
Effective discharge time	85min	60min	65min	35min
Charge efficiency	91%	88%	87%	85.5%
Discharge efficiency	87%	85%	86%	79%
Utilization ratio	0.83	0.78	0.80	0.70

4.2.3 Comparative charge and discharge efficiency

Fig.4.11 determines the comparative thermal performance in term of charge and discharge efficiency. MLSPCM attains the maximum charge efficiency of 91% followed by SLSPCM-1, SLSPCM-2 and SSCB having values of 88%, 87% and 85.5%, respectively. This is due to presence of high melting PCM at the inlet portion, gains the maximum thermal energy from the incoming HTF which helps to enhance the storage capacity of the medium. Also, thermal loses in MLSPCM are minimum which increases the ability to store more energy supplied by HTF. The charge efficiency of SSCB is lowest because the sensible material has less ability to store the energy compared to PCM. However, high temperature difference between PCM and high temperature HTF for SLSPCM-2 results in bigger heat driving force due to which hot region proceeds rapidly. This reduces the storage capacity and decreases the charge efficiency. SLSPCM-1 and MLSPCM both have material with same melting temperature at the top section but in MLSPCM combination of both low and high melting point PCM enhances overall storage potential of the TES system. Similarly, discharge efficiency of MLSPCM, SLSPCM-1 and SLSPCM-2 is higher than SSCB. The reason is that SSCB have no PCM at the outlet section which maintain constant temperature of HTF for some time. Due to continuous decrease in the temperature of sensible medium the discharging time for SSCB is less compared to other TES designs which decreases the overall discharging efficiency. MLSPCM have maximum discharge efficiency of 87% followed by 85%, 86% and 79% for SLSPCM-1, SLSPCM-2 and SSCB, respectively. SLSPCM-2 show better overall discharge performance than SLSPCM-1.

The maximum utilization ratio of 0.83 for MLSPCM TES system show that low solidification temperature PCM at the bottom slow down movement of cold HTF upward and extracts the maximum heat from the PCM. Also, the high solidification temperature PCM at the outlet act as temperature stabilizer for outgoing HTF. This enhances the maximum removal of stored thermal energy. Lowest utilization of SSCB indicates that increase in thermal losses decreases the energy extraction rate of storage medium. SLSPCM-2 have high utilization ratio compared to SLSPCM-1 because low solidification PCM at the outlet creates the thermal buffer effect for longer time and takes time to solidifies which enhances the extraction of energy.



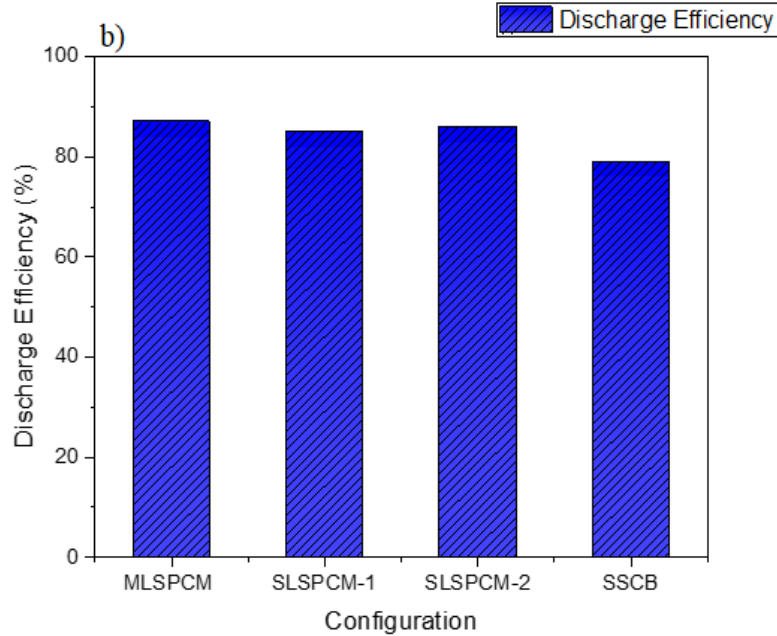


Fig. 4.11. Comparative charge and discharge efficiencies for four different configurations

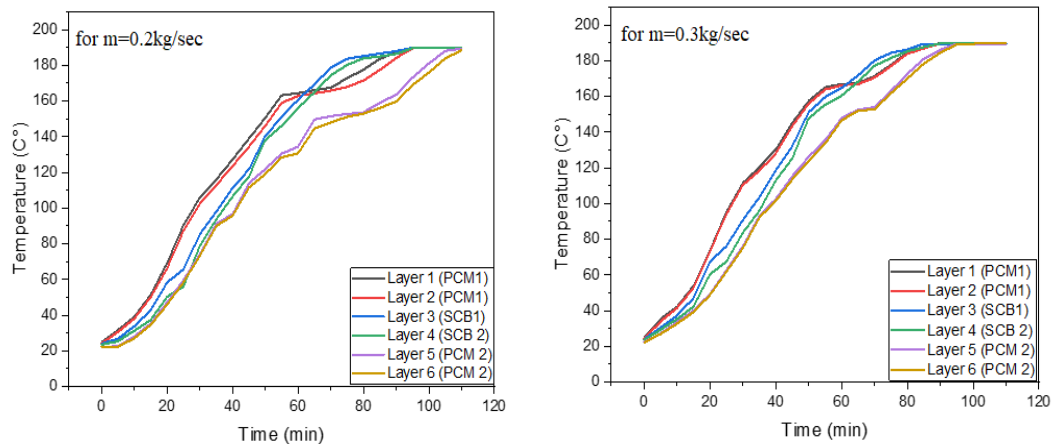
To find out feasible TES alternative, both cost and its behavior during charge and discharge cycles are important to consider. Only sensible heat TES system, i.e., SSCB configuration has low installation cost, but poor charge and discharge performance and low overall energy storage ability makes it less favorable. Whereas SLSPCM-1 and SLSPCM-2 have low-capacity cost, but thermocline performance is not encouraging. While the combined TES design having multilayers of PCM along with low-cost sensible medium, is proved to be most efficient and economical TES choice for medium temperature applications.

4.3 Thermal performance characterization of MLSPCM

In the previous comparative analysis MLSPCM show better charging and discharging performance. Further, in this section effect of changing mass flow rate on thermocline temperature profile, charge, discharge efficiency and variation of fluid temperature at outlet section for MLSPCM configuration is studied.

4.3.1 Thermocline temperature profiles at different mass flow rates

The temperature variation along the axial height of storage tank for different mass flow rates is shown in Fig.4.12. To study the thermal behavior the tank is divided into 6 layers. During charging it is noticed that that for all the flow rates the temperature at the layer close to inlet section rises quickly than the remaining layers. This is because high energy HTF is available at upper section which result in increase in heat transfer between the fluid and PCM at 1st layer. During the initial charging cycles the temperature difference between the top and bottom layer is more but as the heat transfer with the bottom layers increases the temperature gradient decreases. From the temperature curves it is clear that changing the flow rate at the inlet effects the thermal gradient between adjacent layers. Increasing mass flow rate, the thermal gradient between upper and lower layers decreases quickly. This is because the heat transmission between the HTF and storage medium has increased, that result in quick propagation of hot region in downward direction. In case of discharging, the fluid at low temperature come in from the bottom of the storage unit so the temperature at the bottom layer decreases quickly as compared to layers at the top. The results show that increasing the mass flow rate, cold region moves quickly in upward direction, causing the increase in the thermocline thickness. This is because PCM at the bottom solidifies quickly at the increased mass flow rate.



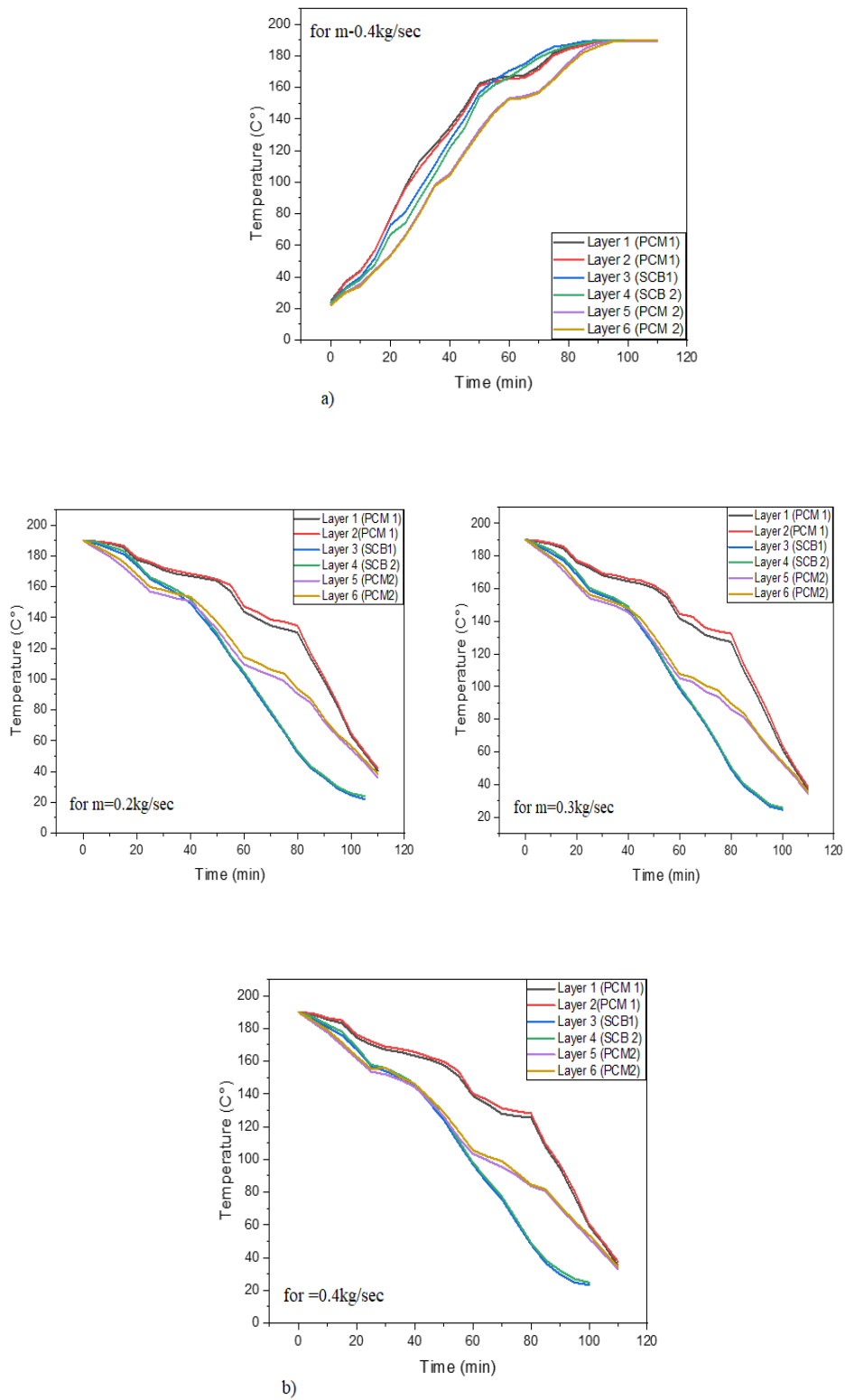


Fig. 4.12. Variation of temperature profiles of MLSPCM storage medium along axial height of tank a) charging b) discharging process

4.3.2 Temperature profiles of fluid and SCB at the center

The comparative thermal curves of fluid at the center of TES unit for different fluid inlet velocities during charging is shown in Fig.4.13. For 0.2kg/sec the fluid reaches to maximum temperature after charging time of 90 min. For the increased flow rates of 0.3kg/sec and 0.4kg/sec the charging time is decreased to 84 min and 79 min respectively. This shows that at higher fluid flow rates the hot region moves quickly downward because of more heat transfer, which reduces effective charging time also.

The comparison between temperature profiles of fluid and concrete for different inlet mass flow rates during discharging at $x = H/2$ is represented in Fig.4.14. The results show that for lower inlet mass flow rate the temperature difference between HTF and concrete decreases after 54 min but for higher flow rates it decreases quickly almost after 50min and 47 min respectively. This is because higher the inlet flow rates enhance the release of stored sensible heat by the storage medium (SCB).

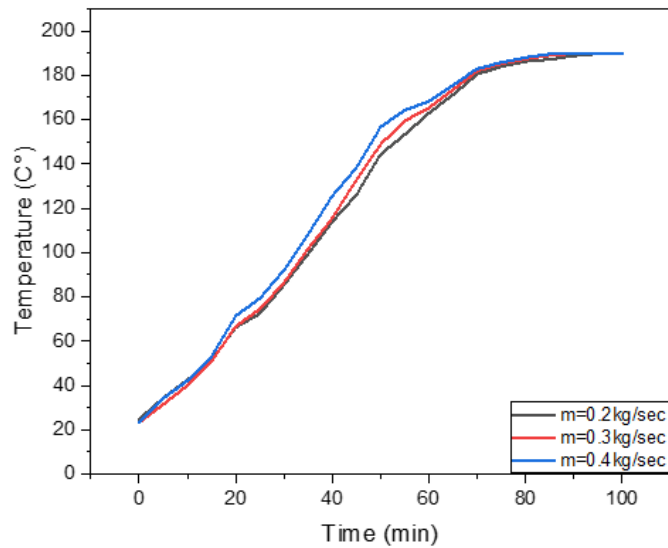


Fig. 4.13. Comparative fluid temperature profile at $x=H/2$ as a function of charging time for different inlet mass flow rates

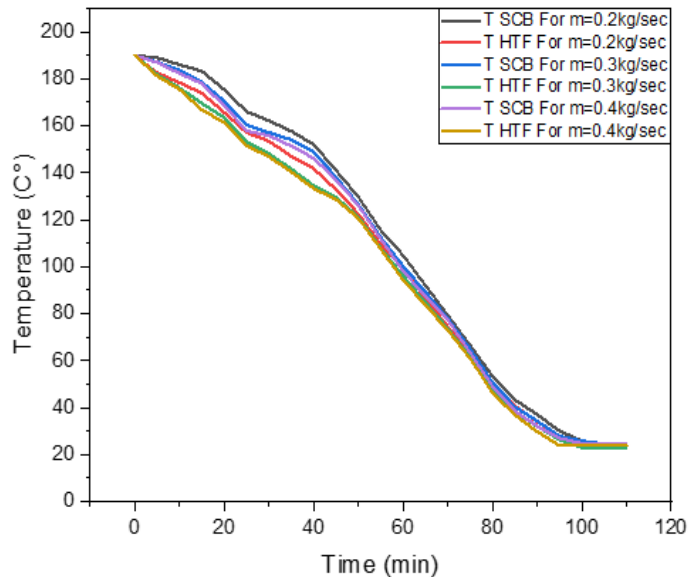


Fig. 4.14. Comparative temperature profiles of HTF and SCB at $x=H/2$ w.r.t discharging time for different inlet mass flow rates

Table 4.2 Performance parameters at different inlet mass flow rates

Parameters	Mass flow rates		
	0.2kgsec	0.3kg/sec	0.4kg/sec
Effective discharge time	75min	68min	62min
Charge efficiency	91%	92%	94%
Discharge efficiency	87%	89%	90%
$E_{f,PCM}$ (after $t=80$ min)	44%	40.2%	38.7%
$E_{f,SCB}$	39%	37.2%	35%

4.3.3 Fluid temperature at outlet for changing mass flow rates

The comparison of fluid temperature at outlet during charging in Fig.4.15 indicates that decreasing the inlet mass flow rate fluid takes more time to transfer heat to the storage media causes the slow increase in fluid outlet temperature. During discharging in Fig.4.15 (b) the temperature of fluid at outlet section is within the acceptable range for longer time. The effective discharge time is more as flow rate is decreased. The reason is that energy extraction rate decreases as fluid mass flow rate decreases. EDT evaluated for 0.2, 0.3 and 0.4kg/sec is 75min, 68min and 62min respectively. Also, at higher flow rates the outlet temperature is stabilized for more time.

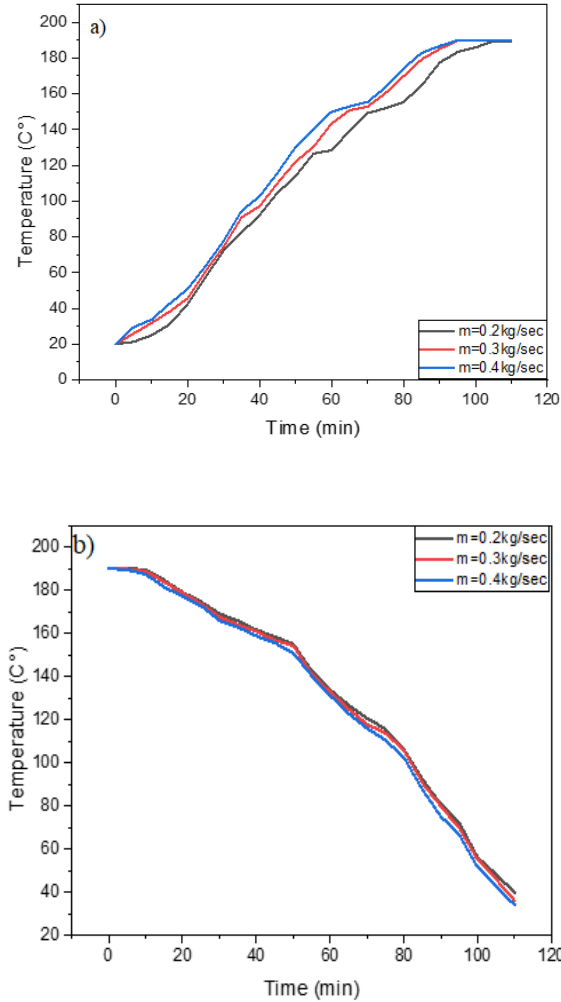


Fig. 4.15. Fluid temperature at outlet section for a) charging b) discharging cycle

4.3.4 Charge and discharge efficiency at different mass flow rates

The change in mass flow rate effects the charging and discharging performance of TES. The results show that during charge process as mentioned in Table 4.2 for higher flow rates the heat transfer coefficient increases i.e., convection heat transfer increases which decreases effective charging time and increases charge efficiency. The maximum charge efficiency for 0.2, 0.3 and 0.4kg/sec is 91%, 92% and 94%. The results indicate that discharge efficiency decreases, and effective discharge time increases as the mass flow rate decreases. This is because lowering the flow rate, heat extraction rate increases and HTF extracts more stored energy. The discharge efficiency is 87%, 89% and 90%. when the mass flow rate is varied to be 0.2, 0.3 and 0.4kg/sec respectively.

4.3.5 Energy removed by HTF during discharging

The results in Fig.4.16 illustrate that more initially stored energy is recovered by HTF in less time at higher inlet flow rates because of quick and more heat transfer. The amount of energy extracted at the end of $t=55\text{min}$ is 80.5%, 83.9% and 90.3% for 0.2, 0.3 and 0.4kg/sec respectively.

4.3.6 Fraction of energy retained by PCM and SCB

Moreover, the fraction of energy retained by the PCM and SCB decreases, as fluid flow rate at inlet section is reduced. This is because the heat exchange between fluid and storage medium is enhanced at the higher mass flow rates and is shown in Table 4.2.

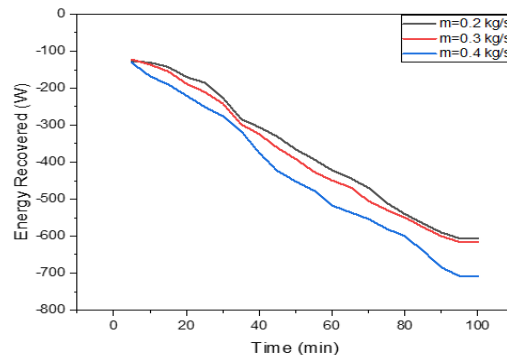


Fig. 4.16. Energy recovered by HTF during discharging for different fluid flow rates

4.3.7 Thermocline thickness for different mass flow rates

The effect of inlet mass flow rate on the formation and degradation of thermocline thickness during discharge process is exhibited in Fig.4.17. It is noticed that initially thermocline thickness is low and as the storage medium releases its stored energy thermocline thickness increases along height of TES tank. The maximum thermocline thicknesses achieved for 0.2, 0.3 and 0.4kg/sec are 0.57, 0.62, 0.63m after the discharging times of 60min, 50min and 40min, respectively. The results show that decreasing the mass flow rate during discharging the convection heat transfer is reduced which results in slow movement of cold region upward and the thermal gradient between different layers is maintained high for the longer period. Similarly, the degradation of the thermocline thickness occurs because of mixing of hot and cold region. Also, it is observed that rapid degradation of thermocline thickness decreases the discharge time due to quick heat release by PCM and SCB.

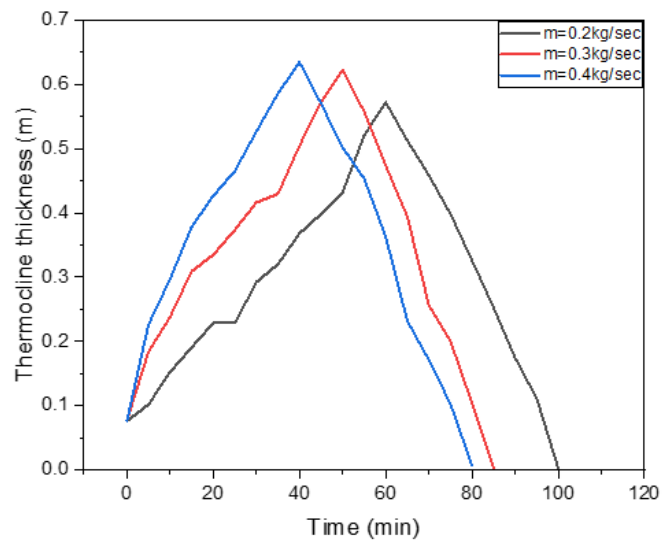


Fig. 4.17. Variation of thermocline thickness w.r.t discharge time at different flow rates

Summary

This section includes the comparative results of charging and discharging behavior for four proposed TES designs based on performance indices thermocline temperature profile, stratification number, temperature of fluid at outlet. Based on these results most economical and efficient TES design is selected for medium temperature application and experiments are performed for selected TES unit. Further, experimental results of proposed design at changing flow rate of fluid at inlet portion are discussed.

Chapter 5

Conclusions & Recommendations

5.1 Conclusions

In the present study, experimental charging and discharging performance of a new type of combined sensible-latent heat configurations for medium temperature is presented. The main idea of current work is to compare charge and discharge behavior of multilayer hybrid TES system with single layer combined TES unit and only sensible energy storage design to propose the more economical and high thermal efficient TES solution. Based on the experimental data stratification in tank, energy transferred and removed by HTF, energy gained and retained by storage material, charge and discharge efficiency, utilization ratio during charge and discharge process is evaluated. Further, effect of changing inlet mass flow rate on thermocline formation and degradation profiles, temperature stabilization at outlet, charge and discharge efficiency, fraction of energy recovered for MLSPCM is studied. The main conclusions are summarized as follows:

- Using multilayer PCM with proper melting temperature in combination with structured sensible heat material enhances the charge and discharge behavior of single tank TES unit.
- The PCM's melting temperature must be selected (decreasing melting point from top to bottom) carefully to take advantage of high energy fluid to enhance storage capacity and removal of maximum stored heat.
- MLSPCM attain the highest energy storage value of 45116.72KJ followed by 38769.03kJ, 37167.2kJ and 31991.57kJ for SLSPCM-1, SLSPCM-2 and SSCB, respectively. It has 14%, 17% and 29% more storage capacity than that of SLSPCM-1, SLSPCM-2 and SSCB, respectively.

- MLSPCM attains highest charging efficiency of 91% followed by SLSPCM-1, SLSPCM-2 and SSCB having 88%, 87% and 85% respectively. MLSPCM and SSCB show maximum and minimum discharge efficiencies of 87% and 79%, respectively.
- It is observed that radial holes in the SCB creates the back flow effect which increases its heat transfer with the HTF.
- In all the combined sensible-latent designs it is not possible to extract the complete stored heat from PCM due to its irregular solidification at sides and in the center.
- Increasing fluid flow rate at inlet increases the heat transmission rate which results in increase in charge and discharge efficiencies. For 0.4kg/sec the charge and discharge efficiencies observed are 94% and 90%. While low flowrates 0.3 and 0.2kg/sec having 92%, 89% and 91%, 87% charge and discharge efficiencies, respectively.

From the above findings it is clear that, using the multilayers of PCM with suitable melting temperatures (decreasing melting points from top to bottom) and low-cost structured concrete (sensible storage medium) is a viable TES solution for medium temperature applications. The proposed hybrid multilayer sensible-latent TES system can be used in cement industry, food, and beverages industry for storing heat and used it further as a process heat in the same industries. Hybrid TES design can be integrated with CSP by changing the temperature range to increase its capacity ratio and cost. This design has no issues of thermal ratcheting like packed bed configurations. However, further study is required to harness the maximum energy of PCM in the proposed hybrid configurations and it's a part of future ongoing research.

5.2 Future recommendations

- Development of numerical models for study on thermal behavior of more practical and large size storage unit.
- Designing of proper fins to enhance heat exchange to harness maximum stored energy of PCM.

Acknowledgements

Thanks to Allah Almighty who gave me strength to complete the work presented in this thesis. I would like to express my sincere gratitude to my supervisor, Dr. Naveed Ahmed for letting me the part of research group at Thermal Energy Lab, USPCAS-E, NUST, Islamabad. I feel privileged to have worked under his kind supervision. He polished my research skills and I have learned a lot under his guidance.

I would like to thank the members of my GEC committee, Prof. Dr. Adeel Waqas, Dr. Majid Ali and Dr. Mariam Mahmood who honored my committee's presence. I would also like to thank my Lab Engineer Mr. Hassan Nazir and Manufacturing Technologist Mr. Qamar-ud-din for their support and guidance throughout my whole work.

I gracefully acknowledge the financial support provided by Research and PGP Directories of USPCASE/NUST.

Appendix-A: Publication

Charging and discharging characterization of novel combined sensible-latent heat TES system by experimental investigation for medium temperature application

Malik Sarmad Zahid^a, Naveed Ahmed^{*a}, Mumtaz A Qaisrani^b, Mariam Mahmood^a, Majid Ali^a, Adeel Waqas^a

^aUS Pakistan Centre for Advanced Studies in Energy (USPCASE), National University of Sciences & Technology (NUST), H-12 Sector, Islamabad, Pakistan.

^bDepartment of Mechanical Engineering, Khwaja Fareed University of Engineering and Information Technology, Rahim Yar Khan 64200, Pakistan

*Corresponding author. E-mail address: Naveed.ahmed@uspcase.nust.edu.pk (Naveed Ahmed).

Abstract

Efficient and economical thermal energy storage (TES) system can effectively reduce mismatch between seasonal energy supply and demand. The single tank type thermocline TES has been investigated as economical alternative for medium temperature applications. However, key disadvantages of this design are quick degradation of thermocline thickness, thermal ratcheting and drop of temperature at outlet section during discharging. To overcome these issues, a new type of structured hybrid sensible-latent design is developed in this research. The focus of the present work is to experimentally investigate the charge and discharge performance of the proposed TES system and it is designed by incorporating the sensible heat concrete block with axial holes placed in between multilayers of PCMs (D- mannitol and adipic acid). Charge and discharge experiments are performed to study the effect of hybrid structured concrete and multilayer PCM's configuration on thermocline temperature profiles, stratification number, total energy stored and retained by storage medium, effective charge and discharge efficiency, utilization ratio. The relative experimental study is developed for four configurations, i.e., multilayered sensible heat concrete with PCM (MLSPCM), two uni-layered sensible concrete with PCM (SLSPCM-1 and SLSPCM-2) arrangements and single sensible heat concrete block (SSCB) arrangement. The results show that effective discharge efficiency

and storage capacity of MLSPCM, SLSPCM-1, SLSPCM-2 and SSCB are 87%, 85%, 86%, 79% and 12.53kWhr, 10.37kWhr, 9.96kWhr, 6.23kWhr, respectively. Moreover, the charging and discharging behavior of MLSPCM is further characterized at different mass flow rates to study the effect on thermocline thickness formation, effective discharge time and amount of energy extracted from storage medium. The present study shows that use of multilayers of PCM with suitable melting and solidification temperature together with low-cost sensible concrete, is viable and economical TES solution for medium temperature applications.

Keywords: Thermal energy storage; medium temperature; thermocline temperature profiles; hybrid multilayered sensible-latent design; structured sensible medium.

Journal: Energy storage

Paper Status: Under Review